Non-Markovian Dynamics of a Damped Driven Two-State System

Pro gradu -tutkielma
Turun yliopisto
Teoreettinen fysiikka
2009
Pinja Haikka
Tarkastajat:
Dos. Sabrina Maniscalco
Prof. Kalle-Antti Suominen

TURUN YLIOPISTO
Fysiikan laitos
HAIKKA, PINJA: Non-Markovian Dynamics of a Damped Driven Two-State System
Pro gradu -tutkielma, 82 s.
Teoreettinen fysiikka
Kesäkuu 2009

Kaikki kvanttimekaaniset systeemit ovat avoimia, eli vuorovaikuttavat ympäristönsä kanssa. Tämän vuorovaikutuksen seurauksena kvanttisysteemi ja sen ympäristö lomittuvat ja kvanttisysteemin liikeyhtälöt muuttuvat oleellisella tavalla. Erityisesti ympäristön vaikutus johtaa dissipatioon ja dekoherensiin eli siihen, että energia ja informaatio siirtyvät kvanttisysteemistä ympäristöön. Tämän prosessin seurauksena kvanttisysteemi menettää kvanttiominaisuutensa. Joissain tapauksissa ympäristöllä on nk. muistiominaisuuksia, joiden ansiosta se voi palauttaa kvanttisysteemille tilapäisesti osan aiemmin menetetystä energiasta ja informaatiosta. Tällaista muistillista systeemiä kutsutaan ei-Markoviseksi systeemiksi.

Tässä tutkielmassa johdetaan ei-Markoviset liikeyhtälöt kaksitasosysteemille, joka vuorovaikuttaa muistillisen ympäristön ja klassisesti kuvaillun laserkentän kanssa. Liikeyhtälöt johdetaan häiriöteoreettisesti heikon kytkennän rajalla. Liikeyhtälöiden ratkaisuja tutkimalla voidaan tarkastella erilaisten approksimaatioiden vaikutusta kvanttisysteemin dynamiikkaan sekä sitä, miten ympäristön muisti ja laserkenttä muuttavat kvanttisysteemin ominaisuuksia. Tämä auttaa ymmärtämään tutkitun systeemin mikroskooppisia fysikaalisia prosesseja ja luo vankan pohjan jatkotutkimukselle.

Tulevaisuudessa tämän tutkielman tuloksia voidaan käyttää tutkittaessa vahvempaa kytkentää kvanttisysteemin ja sen ympäristön välissä, sekä tutkittaessa kvanttitietokoneen loogisten porttien kannalta olennaista sovellutusta, eli kahta laserkenttään kytkettyä kaksitasosysteemiä ja niiden välistä kvanttilomittumista.

Asiasanat: Kvanttimekaniikka, avoimet kvanttisysteemit, ei-Markoviset liikeyhtälöt, dekoherenssi, dissipaatio, kvanttihypyt.

Contents

1 Introduction **1**

2 Derivation of the Master Equation **5**

2.1 General Theory of Quantum Dynamics 5

2.1.1 Pure and Mixed Quantum States 5

2.1.2 Dynamics of Closed Systems 7

2.2 Theory of Open Quantum Systems 9

2.2.1 Reduced Dynamics 9

2.2.2 Lindblad Theorem 10

2.2.3 Interpretation of the Lindblad Form 13

2.3 Microscopic Derivation of the Master Equation 14

2.4 Non-Markovian Master Equation 20

2.4.1 Nakajima-Zwanzig Projection Operator Technique 21

2.4.2 Time-Convolutionless Projection Operator Technique 23

2.5 Comparison Between the Different Approaches 25

3 Master Equation of a Driven Two State System **27**

3.1 The Driven Two-State System 27

3.2 Derivation of the Microscopic Hamiltonian 28

3.2.1 Atom-Field Interactions 29

3.2.2 The Rotating Frame 31
3.3 Master Equation for the Driven Two State System 32
3.3.1 Eigenbasis of the System 33
3.3.2 The Environment 35
3.3.3 Master Equation in the Secular Approximation 36
3.4 The Decay Rates 37
3.5 Decay Rates and the Reservoir Memory 42
3.6 Full Non-Markovian Master Equation 45
3.7 Comparison to Literature 47

4 Dynamics of a Driven Two State System 49
4.1 Optical Bloch Equations 49
4.1.1 Properties of Mappings in the Bloch Ball 51
4.1.2 Dynamics in the Atomic Basis 52
4.2 Relaxation Dynamics 53
4.3 Non-Markovian Dynamics 56
4.4 Full Dynamics of the Driven Two-State System 62
4.4.1 Full Optical Bloch Equations 64
4.4.2 Full Dynamics of the Bloch Vector 65
4.4.3 Dynamics of the Bloch Sphere 70

5 Conclusions 76

Chapter 1

Introduction

Quantum objects can never be described as truly closed systems, i.e., isolated from their environment. Even when the interaction of a quantum system with its environment is weak, the environment alters the dynamics of the quantum system in a fundamental way; eventually energy and information leak from the system to the environment by irreversible dissipative processes [1, 2, 3].

Quantum mechanics also predicts that the interaction with the environment induces decoherence in a quantum system, essentially stripping the system of its "quantumness" [4]. Because quantum technologies, such as quantum computers, quantum cryptographers and other quantum communication devices, exploit quantum properties, the study of the mechanisms of dissipation and decoherence, and their manipulation, has not only fundamental but also applicative value.

In the theory of open quantum systems the quantum system of interest and its environment are considered to be closed system, implying that their combined dynamics is unitary and reversible. Such a total system has a huge, typically infinite, number of degrees of freedom. However, we are generally only interested in the dynamics of the quantum system. Therefore the environmental degrees of freedom are "traced out" and we study the dynamics of the quantum system using a master equation,

i.e., the equation of motion for the reduced density operator describing the quantum system only. The master equation allows us to study dissipative and decoherence processes.

The effects on the system of the interaction with the environment are contained in a so called memory kernel of the master equation. In an exact derivation of the master equation the memory kernel is non-local and the equation is in an integro-differential form, containing an integration over the whole past history of the system. By definition this makes the dynamics of the open system non-Markovian. In many cases the reservoir memory effects occur on a very small timescale and the dynamics can be approximated to be Markovian, i.e., memoryless.

Memory effects, however, are important and interesting from many points of view. During the period of time when the memory effects are not negligible, the flow of energy and information from the system to the environment can be momentarily reversed. The reversal of these processes causes recoherence and restoration of previously lost superpositions [5].

Memory effects are strong in certain types of environments. They are usually characterized by a structured spectral density, meaning that the quantum system interacts more strongly with some modes of the reservoir than with others. Leaky optical cavities and photonic band-gap materials, for example, have such spectral densities [7, 8]. In these physical systems the memory effects can be very considerable and a non-Markovian treatment of the dynamics is inevitable.

In this thesis we study the non-Markovian dynamics of a two-state system driven by a laser and damped by a structured reservoir. This is a fundamental open quantum system model of great interest also for quantum technologies, because it describes a qubit[1] in the presence of an interaction that manipulates coherently its quantum state. The microscopic non-Markovian approach we use allows us to point out the

[1] A qubit is a quantum bit, i.e., it is the basic unit of quantum information.

conditions under which some typical approximations that are often performed in the description of the dynamics of such a system, in particular the secular approximation and the Markovian approximation, break down.

Several physical systems, such as photonic band gap materials, quantum dots, Josephson junctions and other solid state systems have been considered both theoretically and experimentally as possible implementations of qubits and quantum logic gates. Our results constitute a starting point for the description of non-Markovian qubit dynamics in such systems. A natural continuation to this thesis in the future is an extension of our non-Markovian approach to the dissipative dynamics of two driven qubits, focusing on how structured environments may affect the efficiency of the basic logic gates, such as the C-NOT gate and the phase gate [9].

The thesis is organized in the following way. Chapter 2 serves as an introduction to the theory of open quantum systems and its most central results, such as the Lindblad theorem. In chapter 2 we derive a generic master equation under the assumption of a weak coupling between the system and its environment. A Markovian master equation is derived microscopically while a non-Markovian master equation is derived using projection operator techniques.

In chapter 3 we derive the microscopic Hamiltonian and the master equation of the damped driven two-state system. We introduce two types of structured reservoirs, namely the Ohmic reservoir and the Lorentzian reservoir and study the decay rates that they determine. The decay rates essentially control the non-Markovian dynamics of the system.

Chapter 4 is devoted to the study of the dynamics of the damped driven two-state system. We compute the optical Bloch equations of the system using the master equation of chapter 3 and study their solutions numerically. An analytical solution can be found only under some very specific conditions. The dynamics are considered for short and long timescales to shed light on different dynamical effects. Further-

more, we study the solutions of two master equations: the first master equation is valid under the so called secular approximation, which coarse grains some of the intrinsic dynamics of the system, and the second master equation is a more general one, including the effect of the non-secular terms. A comparison between the solutions of the two master equations aims to investigate the conditions of validity of the secular approximation. Finally, chapter 5 summarizes the results and concludes the thesis.

Chapter 2

Derivation of the Master Equation

2.1 General Theory of Quantum Dynamics

2.1.1 Pure and Mixed Quantum States

Pure states of a quantum system are represented by a set of normalized vectors $\{|\psi\rangle \in \mathcal{H} \,|\, ||\psi|| = 1\}$ of a Hilbert space $\mathcal{H}$. These pure states contain all possible information about an isolated quantum object but fail to be sufficient in more complicated circumstances, when it is not possible to assign a single pure state to describe the quantum system. This can happen when the preparation history of the system is unknown, when the system consists of an ensemble of quantum systems or when the quantum object is entangled.

Such situations require a generalization of a pure state, the self-adjoint mixed state density matrix $\rho = \sum_{i,j}^{N} p_{ij} \, |\psi_i\rangle \, \langle\psi_j|$. The space of density matrices is known as the state space of a quantum system,

$$\mathcal{S}(\mathcal{H}) = \{\rho \in L(\mathcal{H}) |\, \rho \geq 0, \, tr(\rho) = 1\}. \tag{2.1}$$

$L(\mathcal{H}) = \{\rho : \mathcal{H} \to \mathcal{H} | \rho \text{ is a bounded operator}\}$ is the space of bounded operators. With $tr(\rho)$ we indicate the trace operation, i.e., the sum of the diagonal elements

of ρ, defined mathematically as $tr(A) = \sum_i \langle\phi_i| A |\phi_i\rangle$. The set $\{|\phi_i\rangle | i \in \mathbb{N}\}$ forms an orthonormal basis of $\mathcal{H}$, i.e., $\langle\phi_i|\phi_j\rangle = \delta_{ij}$ and $\sum_i |\phi_i\rangle \langle\phi_i| = \mathbb{I}$, where $\mathbb{I}$ is the identity operator.

The state space is a convex set, i.e., for any two density matrices ρ_1, $\rho_2 \in \mathcal{S}(\mathcal{H})$ and for any constant $p \in [0, 1]$ we can define a new density matrix $\rho = p\rho_1 + (1 - p)\rho_2$ such that $\rho \in \mathcal{S}(\mathcal{H})$. Pure states cannot be decomposed, i.e., for pure states $p = 1$ and therefore they are the extremities of the set $\mathcal{S}(\mathcal{H})$.

The density matrix has real, non-negative diagonal elements that sum to unity, $\sum_i^N p_{ii} = 1$, where each p_{ii} represents the probability of the quantum system to be in state $|\psi_i\rangle$. The density matrix can be interpreted as a statistical mixture of pure quantum states [10].

The complex valued off-diagonal elements of the density matrix p_{ij}, $i \neq j$, represent coherence between states $|\psi_i\rangle$ and $|\psi_j\rangle$ with the following property: $p_{ij} = p_{ji}^*$. The study of coherence requires care: the density matrix is dependent on the choice of basis vectors and it is always possible to find a basis that diagonalizes ρ and gives the false impression that there is no coherence in the quantum system.

A quantum system in a pure state $|\psi\rangle$ is represented by a density matrix $\rho = |\psi\rangle \langle\psi|$ with $\rho^2 = \rho$. This property is extremely useful to check if a given density matrix represents a pure or a mixed state: it is a necessary and sufficient condition for a pure state. Furthermore, it motivates a measure for the mixedness of a density matrix, namely the *purity*, which is defined as

$$\xi(\rho) \equiv Tr(\rho^2). \tag{2.2}$$

For a pure state the value of purity is maximal, $\xi(|\psi\rangle \langle\psi|) = 1$, otherwise $\xi(\rho) = \sum_i^N p_{ii}^2 < 1$. The value of purity is bounded below by $\frac{1}{N}$, the purity of a maximally mixed state $\rho = \text{diag}(\frac{1}{N}, \cdots, \frac{1}{N})$, where we indicate with $\text{diag}(d_1, d_2, ...)$ a diagonal matrix D with elements d_i equal to $(D)_{ii}$.

Another useful measure for the mixedness of a quantum system is the von Neumann

entropy, a quantum extension of the Shannon entropy, which is defined as

$$S(\rho) \equiv -Tr(\rho \log \rho) = -\sum_i \lambda_i \log \lambda_i, \tag{2.3}$$

where λ_i are the eigenvalues of ρ. The von Neumann entropy takes values between 0 and $\log N$, corresponding to the values of a pure state and a maximally mixed state respectively.

2.1.2 Dynamics of Closed Systems

The dynamics of a quantum system is described by transformations in the state space of the quantum system. It is necessary to require that the transformations conserve the structure of the state space. The general form of such a bijective state transformations is characterized by Wigner's theorem [11].

Theorem 2.1.1 (Wigner's theorem) *Let f be a bijective mapping that conserves convex combinations:*

$$f(p\rho_1 + (1-p)\rho_2) = pf(\rho_1) + (1-p)f(\rho_2), \quad 0 \leq p \leq 1$$

where $\rho_{1,2} \in \mathcal{S}(\mathcal{H})$. Then the mapping is of the form

$$\rho \mapsto f(\rho) = U\rho U^\dagger$$

for a unique (up to a physically irrelevant complex coefficient) unitary (or anti-unitary) operator U.

For a pure state the transformation is $|\psi\rangle \mapsto U|\psi\rangle$. It should be noted that the bijective mapping is invertible and the dynamics described by the mapping is reversible.

To obtain a dynamical transformation for arbitrary times we parametrize the unitary operators as $\{U(t)|t \in \mathbb{R}\}$. The parameterization allows us to introduce the semi-group condition

$$U(t+s) = U(t)U(s). \tag{2.4}$$

The physical meaning of the semi-group condition is that the state of the system at time t is completely determined by the state of the system at time s.
The semi-group condition is used to define a particular form of the unitary operator [12].

Theorem 2.1.2 (Stone's theorem) *Let $\{U(t)|t \in \mathcal{R}\}$ be a continuous set of unitary operators fulfilling the semi-group condition* (2.4)*. Then*

$$U(t) = e^{-itH} \tag{2.5}$$

for a unique Hermitian operator $H = H^\dagger$, called the generator of the semi-group.

When we apply Wigner's and Stone's theorems to physical systems, we find that the generator of the evolution is exactly the Hamiltonian of the system. In this case the unitary operator has to include the physical constant $\hbar$, the Planck constant, which we set to be equal to unity in this thesis.
We have established that the state of a quantum system at some time t is determined by the state at the initial time t_0 as

$$|\psi(t)\rangle = e^{-i(t-t_0)H} |\psi(t_0)\rangle , \tag{2.6}$$

and a formal derivation gives the Schrödinger equation

$$\frac{d}{dt} |\psi(t)\rangle = -iH |\psi(t)\rangle . \tag{2.7}$$

Likewise the density matrix at some time t is determined as

$$\rho(t) = e^{-i(t-t_0)H} \rho(t_0) e^{i(t-t_0)H}, \tag{2.8}$$

and a formal derivation gives the Liouville-von Neumann equation

$$\frac{d}{dt}\rho(t) = -i[H, \rho(t)], \tag{2.9}$$

where $[A, B] = AB - BA$ is the commutator of the operators A and B.

2.2 Theory of Open Quantum Systems

In practice quantum systems are never isolated and the theory of closed quantum systems fails to describe many essential features of quantum dynamics. It is necessary to include the effect of the environment in the dynamical description of the quantum system. However, including the environment in the equation of motion introduces a large, typically an infinite number of degrees of freedom, complicating tremendously the description of the system. Furthermore, one is typically not interested in the dynamics of the environment but rather on its effects on the system. For this reason it it useful to reduce the description of the total closed system to the description of the system of interest only.

2.2.1 Reduced Dynamics

In the theory of open quantum systems one considers a total closed system and separates it into a system of interest, $\mathcal{S}$, and its environment, $\mathcal{E}$. The Hilbert space of the total system is $\mathcal{H} = \mathcal{H}_\mathcal{S} \otimes \mathcal{H}_\mathcal{E}$. If the system and the environment are uncorrelated the density operator of the total system can be written as $\rho = \rho_S \otimes \rho_E$, where ρ_S is the density matrix of the system and ρ_E is the density matrix of the environment.

The dynamics of the closed system is obtained from the Liouville-von Neumann equation. Tracing over the environmental degrees of freedom yields a reduced equa-

tion of motion for the system

$$\frac{d}{dt}\rho_S(t) = -itr_E[H(t), \rho(t)]. \tag{2.10}$$

where

$$\rho_S(t) = tr_E\{\rho(t)\}, \tag{2.11}$$

and $\rho(t)$ is the state of the total system at time t. The reduced equation of motion is exact but it often requires many approximations to obtain an equation that can be solved even numerically.

The solutions of the reduced equation of motion at different times correspond to a dynamical mapping

$$\rho_S(t_0) \mapsto \rho_S(t) = V(t)\rho_S(t_0). \tag{2.12}$$

The mapping describing the evolution of the open system is, in general, no longer unitary. This means that the mapping is generally not reversible and furthermore, positivity of the density matrix is not trivially satisfied. It is also possible that the dynamical mapping no longer satisfies the semi-group condition.

2.2.2 Lindblad Theorem

When the mapping is such that the semi-group condition is fulfilled, $V(s+t) = V(s)V(t)$, a generalization of Stone's theorem[1] states the general form of the dynamical mapping

$$V(t) = e^{\mathcal{L}t} \tag{2.13}$$

for a bounded generator $\mathcal{L}$ [14]. A formal derivation yields the general equation of motion

$$\frac{d}{dt}\rho_S(t) = \mathcal{L}\rho_S(t). \tag{2.14}$$

[1]This result is mathematically formulated by the Hille-Yosida theorem for strongly continuous semigroups [13]. Technical details are not included in this discussion.

The most general form of the generator of the dynamical semi-group $\mathcal{L}$ under certain conditions is stated by the theorems of Lindblad [15] and Gorini, Kossakowski and Sudarshan [16]. For convenience we cite their common result as the Lindblad theorem and the general form of the operator as the Lindblad form. The following presentation of the theorem parallels [17] and citations therein.

The Lindblad form For bounded operators $H = H^\dagger$ and S_k, and positive numbers γ_k the Lindblad form is defined as

$$\mathcal{L}\rho = i[H, \rho] + \sum_k \gamma_k \big(S_k \rho S_k^\dagger - \frac{1}{2}\{S_k^\dagger S_k, \rho\} \big), \tag{2.15}$$

where $\{A, B\} = AB + BA$ is the anti-commutator of operators A and B.

A fundamental assumption of the Lindblad theorem is that the dynamical mapping $V(t)$ is completely positive (CP) [18].

Complete positivity Let $\Phi : \mathcal{A}_1 \to \mathcal{A}_2$ be a linear mapping between two C^*-algebras[2]. The linear mapping can be extended to a mapping $\Phi_n : \mathcal{M}_n(\mathcal{A}_1) \to \mathcal{M}_n(\mathcal{A}_2)$, where $\mathcal{M}_n(\mathcal{A}_i)$ is the space of $n \times n$ matrices with entries from $\mathcal{A}_i$. We identify $(\Phi_n(x))_{ij} = \Phi(a_{ij})$ and define the extension $\Phi_n = \mathbb{I}_n \otimes \Phi$ of Φ.

- If Φ_n is positive for some n, then Φ is n-positive.
- If Φ is *n-positive* for all $n \in \mathbb{N}$, then Φ is completely positive.

Intuitively the concept of CP means that the dynamical mapping can be extended to any larger subspace and the mapping remains positive. It it important to note that a CP mapping is always positive, but the converse is not true in general. The concept of CP is required to define a dynamical semigroup.

[2] C^*-algebras are subsets of bounded operators of a Hilbert space that are closed under additivity and multiplication with both a scalar and another element of the C^*-algebra. A C^*-algebra contains an identity element and an adjoint corresponding to each of its elements.

Dynamical semigroup $\{\Phi(t)|t \geq 0\}$ is a dynamical semi-group when

(i) $\{\Phi(t)|t \geq 0\}$ is a semigroup and

(ii) for each $t \in \mathbf{R}$ the mapping $\Phi(t)$ is completely positive

Within this mathematical framework we are ready to state the Lindblad theorem.

Theorem 2.2.1 (Lindblad theorem) *Let $\mathcal{L}$ be a bounded linear mapping in the space of bounded operators. Then the two following statements are equivalent:*

(i) $\{e^{\mathcal{L}t}|t \geq 0\}$ is a (uniformly) continuous dynamical semigroup

(ii) $\mathcal{L}\rho$ is in the Lindblad form

The Lindblad theorem is a mathematical theorem, but the physical implications are immediate: if a parametrized, completely positive dynamical mapping $V(t)$ fulfills the semi-group condition then we can immediately state the general form of the generator of the semi-group. Namely, the generator is in the Lindblad form. Conversely, if we have an equation of motion in the Lindblad form we are assured that the evolution of the density matrix is always physical as a direct consequence of complete positivity and positivity.

An important detail in the Lindblad theory is that the operators H and S_k are bounded. In particular H is interpreted physically as the Hamiltonian of a quantum system and in many physical situations, such as in the description of a quantum harmonic oscillator, the Hamiltonian is unbounded. A Lindblad theorem for unbounded operators does not exist.

The range of applicability of the Lindblad theorem seems quite restricted, but we will see that a number of well-motivated approximations in a microscopic derivation of the master equation can be used to cast the equation of motion of the reduced density matrix (2.10) into the Lindblad form.

2.2.3 Interpretation of the Lindblad Form

A master equation in the Lindblad form has a physical interpretation that can be understood in terms of the so called quantum jumps, which we briefly recall here [19, 20].

Let us consider a quantum system in a pure state $|\Psi\rangle$ evolving during a small interval of time Δt according to one of the following processes:

(1) A quantum jump determined by an operator A:

$$|\Psi(t)\rangle \mapsto |\Psi(t+\Delta t)\rangle_{QJ} = \frac{A\,|\Psi(t)\rangle}{||A\,|\Psi(t)\rangle\,||} \tag{2.16}$$

with a probability of $\Delta P = \langle\Psi(t)|\,A^\dagger A\,|\Psi(t)\rangle\,\gamma\Delta t$, where γ is a positive constant.

(2) Unitary evolution generated by an effective non-Hermitian Hamiltonian $H_{\text{eff}} = H - \frac{i}{2}\gamma A^\dagger A$

$$|\Psi(t)\rangle \mapsto |\Psi(t+\Delta t)\rangle_U = \frac{e^{-iH_{\text{eff}}\Delta t}\,|\Psi\rangle}{||e^{-iH_{\text{eff}}\Delta t}\,|\Psi\rangle\,||} \tag{2.17}$$

with a probability of $1-\Delta P$.

These two processes amount to the following change of the density matrix corresponding to the state vector:

$$\begin{aligned} |\Psi(t)\rangle\langle\Psi(t)| &\mapsto |\Psi(t+\Delta t)\rangle\langle\Psi(t+\Delta t)| \\ &= \Delta P\,|\Psi(t+\Delta t)\rangle_{QJ\,QJ}\langle\Psi(t+\Delta t)| \\ &\quad +(1-\Delta P)\,|\Psi(t+\Delta t)\rangle_{U\,U}\langle\Psi(t+\Delta t)|\,. \end{aligned} \tag{2.18}$$

We consider a Monte Carlo wave function process to simulate the evolution of the state vector, where at each interval of time a random number $r \in [0,1]$ is compared to the probability ΔP to determine which process, (1) or (2), takes place: when $r < \Delta P$ the state vector undergoes a quantum jump and when $r \geq \Delta P$ the state vector evolves deterministically.

When this simulation process is performed for a large ensemble of state vectors, we obtain from (2.18), in the limit $\Delta t \to 0$, a master equation

$$\frac{d\rho}{dt} = -i[H,\rho] + \gamma\big(A\rho A^\dagger - \frac{1}{2}\{A^\dagger A, \rho\}\big), \tag{2.19}$$

which is in the Lindblad form, where $\rho = \frac{1}{N}\sum_i^N |\Psi\rangle_{ii}\langle\Psi|$ and N is the number of state vectors forming the ensemble.

This simple study shows that a master equation in the Lindblad form describes the dynamics of a quantum system whose deterministic evolution is disrupted by quantum jumps. The constant γ is interpreted as the decay rate of that particular quantum jump channel. This result can be generalized to include more than one jump channel.

2.3 Microscopic Derivation of the Master Equation

To fully incorporate all physically relevant effects to the dynamics of the reduced density matrix we must derive the master equation starting from the Lioville-von Neumann equation for the total closed system with the appropriate Hamiltonian for the system, the environment and their interaction.

We begin the derivation by decomposing the Hamiltonian of the total system:

$$H(t) = H_S \otimes \mathbb{I}_E + \mathbb{I}_S \otimes H_E + \alpha H_I(t), \tag{2.20}$$

where H_S and H_E are the free Hamiltonians of the system and the environment respectively and $H_I(t)$ is the interaction Hamiltonian with α, a dimensionless constant.

For convenience we consider the dynamics in the interaction picture. A transformation to the interaction picture changes the interaction Hamiltonian and the density

matrix of the total system to

$$\begin{aligned} \tilde{H}_I(t) &= e^{it(H_S+H_E)} H_I(t) e^{-it(H_S+H_E)}, \\ \tilde{\rho}(t) &= e^{it(H_S+H_E)} \rho(t) e^{-it(H_S+H_E)}, \end{aligned} \tag{2.21}$$

where tildes are used to identify quantities in the interaction picture.
The Liouville-von Neumann equation in the interaction picture is

$$\frac{d}{dt}\tilde{\rho}(t) = -i\alpha \left[\tilde{H}_I(t), \tilde{\rho}(t)\right]. \tag{2.22}$$

The advantage of interaction picture is now apparent; we only have to consider the interaction Hamiltonian.
The Liouville-von Neumann equation can be formally integrated to obtain

$$\tilde{\rho}(t) = \tilde{\rho}(t_0) - i\alpha \int_{t_0}^{t} ds \left[\tilde{H}_I(s), \tilde{\rho}(s)\right]. \tag{2.23}$$

The integral form of Eq. (2.23) can be substituted into the differential form of Eq. (2.22) and iterated to obtain an exact equation of motion

$$\frac{d}{dt}\tilde{\rho}(t) = -i\alpha \left[\tilde{H}_I(t), \tilde{\rho}(t_0)\right] - \alpha^2 \int_{t_0}^{t} ds \left[\tilde{H}_I(t), [\tilde{H}_I(s), \tilde{\rho}(t_0)]\right] + \mathcal{O}(\alpha^3). \tag{2.24}$$

Next we trace over the environmental degrees of freedom and make a technical assumption $tr_E[\tilde{H}_I(t), \tilde{\rho}(t_0)] = 0$.

Approximation 1: *Weak coupling*

We assume that the coupling between the system and its environment is weak, i.e., the coupling constant $\alpha \ll 1$. This allows us to neglect all terms $\mathcal{O}(\alpha^3)$. This approximation is known as the Born or the weak coupling approximation.
We also assume that the system is initially uncorrelated $\tilde{\rho}(t_0) = \tilde{\rho}_S(t_0) \otimes \tilde{\rho}_E(t_0)$. The assumption of factorized initial conditions is justified in the weak-coupling regime

when the system can be prepared to a state that is not correlated with the environment.

As a consequence of weak coupling we can also assume that the state of the reservoir is not affected by the interaction with the system. This means that $\tilde{\rho}_E(t) = \tilde{\rho}_E(t_0) \equiv \tilde{\rho}_E$ for all times $t \geq t_0$.

Equation (2.24) depends on the initial state of the system. However, it is easy to see from (2.23) that the changes in the state of the system are small, namely $|\rho_S(t) - \rho_S(t_0)| = \mathcal{O}(\alpha)$. Therefore in the weak coupling regime it is justified to replace the initial state by the current state of the system to yield the Redfield master equation

$$\frac{d}{dt}\tilde{\rho}_S(t) = -\int_{t_0}^{t} ds\, tr_E \left[\tilde{H}_I(t), [\tilde{H}_I(s), \tilde{\rho}_S(t) \otimes \tilde{\rho}_E]\right]. \tag{2.25}$$

For the sake of readability the coupling constant has now been incorporated into the interaction Hamiltonian.

We continue by decomposing the interaction Hamiltonian to

$$H_I = S \otimes E, \tag{2.26}$$

where $S \in \mathcal{H}_\mathcal{S}$ and $E \in \mathcal{H}_\mathcal{E}$.

A discrete system Hamiltonian has a set of eigenvalues $\{\epsilon_i\}$ and a set of corresponding eigenvectors $\{|\psi_i\rangle\}$ that fulfill the eigenvalue problem

$$H_S |\psi\rangle = \epsilon |\psi\rangle . \tag{2.27}$$

The eigenvectors are used to define the eigenoperators of S appearing in Eq. (2.26). The eigenoperators are

$$S(\omega) = \sum_{\omega=\epsilon'-\epsilon} |\psi\rangle \langle\psi| S |\psi'\rangle \langle\psi'| . \tag{2.28}$$

and they have two important properties, namely that they sum to the original operator,

$$S = \sum_{\omega} S(\omega), \tag{2.29}$$

and that their commutation relations with H_S are

$$\begin{aligned} \left[H_S, S(\omega)\right] &= -\omega S(\omega) \\ \left[H_S, S^\dagger(\omega)\right] &= \omega S^\dagger(\omega). \end{aligned} \tag{2.30}$$

These properties allow an easy transformation to the interaction picture

$$\tilde{S}(t) = e^{iH_S t} S e^{-iH_S t} = \sum_\omega e^{-i\omega t} S(\omega). \tag{2.31}$$

The interaction Hamiltonian in the interaction picture is

$$\tilde{H}_I(t) = \tilde{S}(t) \otimes \tilde{E}(t) = \sum_\omega e^{-i\omega t} S(\omega) \otimes \tilde{E}(t), \tag{2.32}$$

where

$$\tilde{E}(t) = e^{iH_E t} E e^{-iH_E t}. \tag{2.33}$$

Inserting the interaction Hamiltonian (2.32) into the Redfield master equation (2.25) we obtain

$$\frac{d}{dt}\tilde{\rho}_S(t) = \sum_{\omega,\omega'} \Gamma_\omega(t) e^{i(\omega-\omega')t} \left[S^\dagger(\omega) S(\omega') \tilde{\rho}_S(t) - S^\dagger(\omega) \tilde{\rho}_S(t) S(\omega')\right] + H.c. \tag{2.34}$$

where $H.c.$ indicates the Hermitian conjugation and we have defined

$$\Gamma_\omega(t) = \int_0^{t-t_0} d\tau e^{-i\omega\tau} tr_E\{\tilde{E}^\dagger(t)\tilde{E}(t-\tau)\tilde{\rho}_E\}. \tag{2.35}$$

The quantity

$$tr_E\{\tilde{E}^\dagger(t)\tilde{E}(t-\tau)\tilde{\rho}_E\} \tag{2.36}$$

is the reservoir correlation function. For an environment in a stationary state, $[H_E, \rho_E] = 0$, the correlation function is invariant under time-translations. Therefore we consider $tr_E\{\tilde{E}^\dagger(\tau)\tilde{E}(0)\tilde{\rho}_E\}$ instead of the reservoir correlation function of Eq. (2.36).

Approximation 2: ***Markovian approximation***

In many physical systems the reservoir correlation function decays over a time τ_C, which is known as the reservoir correlation time. This time is typically small compared to the relaxation time τ_R, which is used as a measure of the timescale of appreciable changes in the state of the system. Indeed, when this is the case, i.e., $\tau_C \ll \tau_R$, we may perform the Markov approximation and replace the upper limit of integration of Eq. (2.35) by infinity. In this case Eq. (2.35) becomes the Fourier transform of the reservoir correlation function and it is no longer time-dependent.
Markovian dynamics are, by definition, memoryless. A common misconception is that a non-Markovian master equation must contain an integration over the whole past history of the system. Clearly the Redfield master equation is not in such form, yet it is legitimate to state that it becomes a Markovian master equation only once the Markovian approximation has been made. This question is addressed in Sec. 2.5.
It it worth noting that the semi-group condition is closely connected to the Markovian dynamics. When the dynamical mapping fulfills the semi-group condition, the system cannot carry any information about past states, i.e., there cannot be any memory effects. Then a non-Markovian system does not fulfill the conditions of the Lindblad theorem.

Approximation 3: ***Secular approximation***

We define the typical value of $|\omega - \omega'|^{-1}$, with $\omega \neq \omega'$ as the typical timescale τ_S of the system. This quantity sets the timescale of the intrinsic evolution of the system. When τ_S is small compared to the relaxation timescale τ_R then the effect of

the intrinsic evolution averages out and we may perform the secular approximation. The secular approximation comprises of neglecting the non-secular terms, i.e. the rapidly oscillating terms proportional to $e^{\pm it/\tau_S}$ in Eq. (2.34).

In the last step of the derivation of the master equation the integral over the reservoir correlation function is divided into real and imaginary parts, $\Gamma_\omega = \frac{1}{2}\gamma_\omega + i\lambda_\omega$. After a straightforward calculation, transforming back to the Schrödinger picture, we find the Born-Markov master equation

$$\frac{d}{dt}\tilde{\rho}_S(t) = -i\left[H_S + H_{LS}, \rho_S(t)\right] + \sum_\omega \gamma_\omega \left(S(\omega)\rho_S(t)S^\dagger(\omega) - \frac{1}{2}\{S^\dagger(\omega)S(\omega), \rho_S(t)\}\right), \tag{2.37}$$

where we have defined the Lamb shift Hamiltonian as

$$H_{LS} = \sum_\omega \lambda_\omega S^\dagger(\omega)S(\omega). \tag{2.38}$$

We have successfully derived a master equation in the Lindblad form using the following approximations: weak coupling, memoryless dynamics and small timescale intrinsic evolution in comparison with relaxation dynamics, as well as the assumptions of factorized initial conditions and a stationary reservoir.

The first term of the master equation describes the unitary evolution of the system generated by the system Hamiltonian. The Lamb shift Hamiltonian introduces a small shift in the eigenstates of the system but has no qualitative effect on the dynamics. In many cases the Lamb shift Hamiltonian is neglected.

The sum term in the right hand side (r.h.s) of Eq. (2.37) contains the dissipative dynamics of the systems, i.e., the direct effect of the interaction between the system and the environment. It describes both the dynamics of dissipation, i.e. leaking of energy from the system to the environment and the dynamics of decoherence, i.e. the loss of quantum coherence. Each term of the sum is in the Lindblad form and we can interpret the loss of energy and information to be a result of quantum jumps generated by the operators $S(\omega)$ at decay rates γ_ω respectively.

2.4 Non-Markovian Master Equation

The master equation (2.37) derived in the previous section is Markovian and valid in the weak coupling regime. A rigorous approach to non-Markovian dynamics employs *projection operator techniques* (POT) [21, 22, 23, 24]. The underlying idea of POTs is to divide a total, closed system into a relevant part (the system of interest) and an irrelevant part (the environment). A projection super-operator $\mathcal{P}$ is used to obtain the relevant part of the total density matrix ρ

$$\mathcal{P}\rho = tr_E\{\rho\} \otimes \rho_E = \rho_S \otimes \rho_E, \tag{2.39}$$

where ρ_E is the reference state, e.g., a thermal state in equilibrium. POTs provide a solid framework for the study of dynamics beyond the Born and the Markov approximations.

The projection operator has a complement $\mathcal{Q} \equiv \mathbb{I} - \mathcal{P}$, which is also a projection operator, acting on ρ to give the irrelevant part $\mathcal{Q}\rho = \rho - \mathcal{P}\rho$.

Stated below is a list of properties of the projection operator and its complement:

$$\mathcal{P} + \mathcal{Q} = \mathbb{I} \tag{2.40}$$

$$\mathcal{P}^2 = \mathcal{P} \tag{2.41}$$

$$\mathcal{Q}^2 = \mathcal{Q} \tag{2.42}$$

$$\mathcal{P}\mathcal{Q} = 0 = \mathcal{Q}\mathcal{P}. \tag{2.43}$$

The starting point of the derivation of the non-Markovian master equation is once more the Liouville-von Neumann equation of the total closed system in the interaction picture:

$$\frac{d}{dt}\rho(t) = -i\alpha[H_I(t), \rho(t)] \equiv \alpha\mathcal{L}(t)\rho(t), \tag{2.44}$$

where the super-operator $\mathcal{L}(t)$ is the Liouvillean and the dimensionless constant α has been introduced to represent the strength of the coupling between the system and the environment.

The whole derivation is performed in the interaction picture but to simplify the notation we will omit the use of tildes to indicate the interaction picture quantities.

2.4.1 Nakajima-Zwanzig Projection Operator Technique

A projection on the relevant and the irrelevant Hilbert spaces yields two equations of motion

$$\frac{d}{dt}\mathcal{P}\rho = \mathcal{P}\frac{d}{dt}\rho = \alpha\mathcal{P}\mathcal{L}(t)\rho(t) = \alpha\mathcal{P}\mathcal{L}(t)\mathcal{P}\rho(t) + \alpha\mathcal{P}\mathcal{L}(t)\mathcal{Q}\rho(t), \tag{2.45}$$

$$\frac{d}{dt}\mathcal{Q}\rho = \mathcal{Q}\frac{d}{dt}\rho = \alpha\mathcal{Q}\mathcal{L}(t)\rho(t) = \alpha\mathcal{Q}\mathcal{L}(t)\mathcal{P}\rho(t) + \alpha\mathcal{Q}\mathcal{L}(t)\mathcal{Q}\rho(t), \tag{2.46}$$

where, in the last equality, we used the property (2.40).

The equation of motion of the irrelevant part is formally integrated to yield

$$\mathcal{Q}\rho(t) = \mathcal{G}(t,t_0)\mathcal{Q}\rho(t_0) + \alpha\int_{t_0}^{t} ds\,\mathcal{G}(t,s)\mathcal{Q}\mathcal{L}(s)\mathcal{P}\rho(s). \tag{2.47}$$

We have introduced a propagator

$$\mathcal{G}(t,s) = T_{\leftarrow}\exp\{\alpha\int_{s}^{t} ds'\mathcal{Q}\mathcal{L}(s')\}, \tag{2.48}$$

for which

$$\frac{d}{dt}\mathcal{G}(t,s) = \alpha\mathcal{Q}\mathcal{L}(t)\mathcal{G}(t,s), \quad \mathcal{G}(s,s) = \mathcal{I}. \tag{2.49}$$

The time-ordering operator $T_{\leftarrow}$ ensures a correct chronological structure of the generator.

When $\mathcal{Q}\rho(t)$ is inserted into the equation of motion (2.45) of the relevant part we obtain the Nakajima-Zwanzig equation

$$\frac{d}{dt}\mathcal{P}\rho = \alpha\mathcal{P}\mathcal{L}(t)\mathcal{G}(t,t_0)\mathcal{Q}\rho(t_0) + \alpha\mathcal{P}\mathcal{L}(t)\mathcal{P}\rho(t) + \alpha^2\int_{t_0}^{t}\mathcal{P}\mathcal{L}(t)\mathcal{G}(t,s)\mathcal{Q}\mathcal{L}(s)\mathcal{P}\rho(s). \tag{2.50}$$

The Nakajima-Zwanzig equation is an exact integro-differential equation of motion for the relevant part of a closed system. However, it is instructive to simplify it further with the technical assumption that was already introduced in the microscopic derivation: $tr_E[H_I(t), \rho(t_0)] = 0$. This leads to $\mathcal{PL}(t)\mathcal{P} = 0$ and removes the second term from the r.h.s of Eq. (2.50).

Furthermore, assuming factorized initial conditions $\rho(t_0) = \rho_S(t_0) \otimes \rho_E(t_0)$ is equivalent to $\mathcal{P}\rho(t_0) = \rho(t_0)$ and leads to $\mathcal{Q}\rho(t_0) = 0$. Thus the first term of the r.h.s of Eq. (2.50) vanishes too.

Consequently the Nakajima-Zwanzig equation for factorized initial conditions is

$$\frac{d}{dt}\mathcal{P}\rho(t) = \int_{t_0}^{t} ds\, \mathcal{K}(t,s)\mathcal{P}\rho(s), \tag{2.51}$$

where we have defined a memory kernel

$$\mathcal{K}(t,s) = \alpha^2 \mathcal{P}\mathcal{L}(t)\mathcal{G}(t,s)\mathcal{L}(s)\mathcal{P}. \tag{2.52}$$

A series expansion of the propagator with respect to the coupling constant yields an expansion of the memory kernel

$$\begin{aligned} \mathcal{K}(t,s) &= \alpha^2 \mathcal{P}\mathcal{L}(t)\mathcal{Q}\mathcal{L}(s)\mathcal{P} + \mathcal{O}(\alpha^3) \\ &= \alpha^2 \mathcal{P}\mathcal{L}(t)\mathcal{L}(s)\mathcal{P} + \mathcal{O}(\alpha^3), \end{aligned} \tag{2.53}$$

where the last equality combines (2.40) and the technical assumption $\mathcal{PL}(t)\mathcal{P} = 0$. We use the weak coupling assumption and neglect all terms $\mathcal{O}(\alpha^3)$. In this regime the Nakajima-Zwanzig equation takes the form

$$\frac{d}{dt}\mathcal{P}\rho = \alpha^2 \int_{t_0}^{t} ds\, \mathcal{P}\mathcal{L}(t)\mathcal{L}(s)\mathcal{P}\rho(s), \tag{2.54}$$

and the equation of motion for the relevant part ρ_S is

$$\frac{d}{dt}\rho_S(t) = -\alpha^2 \int_{t_0}^{t} ds\, tr_E\big[H_I(t), [H_I(s), \rho_S(s) \otimes \rho_E]\big]. \tag{2.55}$$

This master equation includes an integration over the whole history of the density matrix of the relevant part.

2.4.2 Time-Convolutionless Projection Operator Technique

The time-convolutionless (TCL) POT, as suggested by its name, removes the time-convolution from the Nakajima-Zwanzig equation, resulting in a time-local master equation.

The starting point of TCL is the formal solution of the equation of motion of the irrelevant part of the density matrix, Eq. (2.47), rewritten as

$$\mathcal{Q}\rho(t) = \mathcal{G}(t,t_0)\mathcal{Q}\rho(t_0) + \alpha \int_{t_0}^{t} ds\, \mathcal{G}(t,s)\mathcal{Q}\mathcal{L}(s)\mathcal{P}G(t,s)(\mathcal{Q}+\mathcal{P})\rho(t). \tag{2.56}$$

In the above equations the backwards propagator

$$G(t,s) = T_{\rightarrow} \exp\{-\alpha \int_{s}^{t} ds' \mathcal{L}(s')\} \tag{2.57}$$

was introduced and used to rewrite $\rho(s)$ as

$$\rho(s) = G(t,s)\rho(t). \tag{2.58}$$

Furthermore, we define an auxiliary quantity

$$\Sigma(t) = \alpha \int_{t_0}^{t} ds\, \mathcal{G}(t,s)\mathcal{Q}\mathcal{L}(s)\mathcal{P}G(t,s) \tag{2.59}$$

to rewrite Eq. (2.56) as

$$[1-\Sigma(t)]\mathcal{Q}\rho(t) = \mathcal{G}(t,t_0)\mathcal{Q}\rho(t_0) + \Sigma(t)\mathcal{P}\rho(t). \tag{2.60}$$

The quantity $1-\Sigma(t)$ may be inverted when the coupling constant α and/or the interval of time $[t_0,t]$ is small. When these conditions hold, $[1-\Sigma(t)]^{-1}$ exists and the irrelevant part of the total density matrix is

$$\mathcal{Q}\rho(t) = [1-\Sigma(t)]^{-1}\mathcal{G}(t,t_0)\mathcal{Q}\rho(t_0) + [1-\Sigma(t)]^{-1}\Sigma(t)\mathcal{P}\rho(t). \tag{2.61}$$

This equation is inserted into the equation of motion for the relevant part, Eq. (2.45), giving

$$\frac{d}{dt}\mathcal{P}\rho(t) = \mathcal{K}(t)\mathcal{P}\rho(t) + \mathcal{I}(t)\mathcal{Q}\rho(t_0), \tag{2.62}$$

where we have defined the TCL generator and the inhomogeneity term, respectively, as

$$\mathcal{K}(t) = \alpha\mathcal{P}\mathcal{L}(t)[1-\Sigma(t)]^{-1}\mathcal{P}, \tag{2.63}$$

$$\mathcal{I}(t) = \alpha\mathcal{P}\mathcal{L}(t)[1-\Sigma(t)]^{-1}\mathcal{G}(t_0,t)\mathcal{Q}. \tag{2.64}$$

The usual assumption of factorized initial conditions sets the inhomogeneity term of the above equation to zero.

A remarkable feature of this equation of motion is that it is exact but local in time. The coupling constant was assumed to be small and this property is further exploited in a perturbative treatment of equation (2.62).

Perturbation expansion of the TLC generator

Let us assume that the operator $[1-\Sigma(t)]^{-1}$ exists and it is expanded to a converging series

$$[1-\Sigma(t)]^{-1} = \sum_{n=0}^{\infty}\Sigma(t)^n. \tag{2.65}$$

Then the TCL generator is

$$\begin{aligned}\mathcal{K}(t) &= \alpha\sum_{n=0}^{\infty}\mathcal{P}\mathcal{L}(t)\Sigma(t)^n\mathcal{P} \\ &\equiv \sum_{n=1}^{\infty}\alpha^n\mathcal{K}_n(t).\end{aligned} \tag{2.66}$$

We further expand

$$\Sigma(t) = \sum_{n=1}^{\infty}\alpha^n\Sigma_n(t) \tag{2.67}$$

and insert this expansion into Eq. (2.66).

As before, we neglect all terms $\mathcal{O}(\alpha^3)$. Comparing similar terms in the expansions we obtain the first two terms of the generator:

$$\mathcal{K}_1(t) = \mathcal{P}\mathcal{L}(t)\mathcal{P} = 0, \tag{2.68}$$

$$\mathcal{K}_2(t) = \mathcal{P}\mathcal{L}(t)\Sigma_1(t)\mathcal{P} = \int_{t_0}^{t} ds\,\mathcal{P}\mathcal{L}(t)\mathcal{L}(s)\mathcal{P}. \tag{2.69}$$

The technical assumption that was used in the Nakajima-Zwanzig POT sets the first term to zero. The form of the second term is obtained from the Taylor expansions of the propagator $\mathcal{G}(t,s)$ and of the backwards propagator $G(t,s)$.
Using Eqs. (2.63) and (2.64) and the results above we obtain from Eq. (2.62) the time-convolutionless master equation to the second order in perturbation theory, i.e., the TCL2 master equation:

$$\frac{d}{dt}\rho_S(t) = -\int_{t_0}^{t} ds\, tr_E \left[H_I(t), [H_I(s), \rho_S(t) \otimes \rho_E]\right]. \tag{2.70}$$

2.5 Comparison Between the Different Approaches

We have derived a non-Markovian master equation in the weak coupling regime using two variants of the projection operator techniques, namely the Nakajima-Zwanzig POT and the time-convolutionless POT. Both derivations assumed a stationary reservoir and factorized initial conditions.
The main difference in these approaches is that the TCL2 master equation (2.70) is in a time local form whereas the Nakajima-Zwanzig master equation (2.55) requires an integration over the history of the system. However, since both approaches rely on the same assumptions and approximations, *we expect them to describe the approximated dynamics with the same accuracy in the weak coupling regime.* In fact, it has been argued by Royer [26] in a lengthy calculation, that in the limit of weak coupling between the system and the environment a time-local master equation (such as the TCL2 master equation) is, in fact, generally *more* accurate than a "memory" equation (such as the Nakajima-Zwanzig equation).
This observation shows that local in time master equations can be non-Markovian and there does not need to be a memory kernel or integration over the history of the system to describe memory effects. Indeed there are cases, such as a two state system dissipating into an environment of arbitrary spectral density, where the exact

and therefore non-Markovian master equation is of the time-convolutionless form [1, 25].

Finally we note that the TCL2 master equation coincides exactly with the Born master equation (2.25), and it can be further decomposed using the methods presented in the microscopic derivation. The reservoir memory is then embedded in the time-dependence of the decay rates. In the next chapter we will investigate how the time-dependent decay rates can cause memory effects, focusing on a specific physical system of interest.

Chapter 3

Master Equation of a Driven Two State System

3.1 The Driven Two-State System

In the rest of the thesis we will study the non-Markovian dynamics of a driven two-state system. The open quantum system of interest consists of a two-level atom with an energy separation ω_A interacting with a monochromatic laser of frequency ω_L almost resonant with the Bohr frequency ω_A of the atom, $|\omega_L - \omega_A| \ll \omega_A$. Larger detunings affect other levels of the atom and near-resonance is needed to be able to treat the atom as a two-state system [27].

The atom also interacts with an electromagnetic field modelled as an infinite chain of quantum harmonic oscillators. We focus here on environments that have a structured spectral distribution, i.e. the system interacts in a stronger way with some modes of the reservoir and in a weaker way with others. In particular we consider two types of environment: an Ohmic reservoir and a Lorentzian reservoir.

An atom interacting with a near-resonant driving field exhibits oscillations in its excited state population at the so-called Rabi frequency Ω. Furthermore, when the

atom interacts with the modes of the electromagnetic field, the atomic excitations decay into the environment as fluorescent scattering, damping the Rabi oscillations. The spectrum of the scattered light does not match the spectrum of the laser because it is modified by the interaction with the atom. The emitted spectrum has two sidebands at $\Omega_L \pm \Omega$ in addition to the main frequency Ω_L of the laser: this structure is known as the Mollow triplet [28]. Furthermore, a study of the scattered light shows that it is anti-bunched and therefore non-classical [29, 30].

This phenomenon, known as resonance fluorescence, has been widely studied (See, e.g., [31] and references therein), especially in the Markovian regime. The next two chapters aim to shed some light on the first non-Markovian corrections to the dynamics of the atom in the weak coupling regime.

3.2 Derivation of the Microscopic Hamiltonian

We introduce the Pauli matrices

$$\sigma_x = \begin{pmatrix} 0 & 1 \\ 1 & 0 \end{pmatrix}, \quad \sigma_y = \begin{pmatrix} 0 & -i \\ i & 0 \end{pmatrix}, \quad \sigma_z = \begin{pmatrix} 1 & 0 \\ 0 & -1 \end{pmatrix}. \tag{3.1}$$

In the atomic basis $\{|e\rangle, |g\rangle\}$, where $|e\rangle$ is the excited state of the atom and $|g\rangle$ is the ground state, the Pauli matrices have a representation $\sigma_x = |e\rangle\langle g| + |g\rangle\langle e|$, $\sigma_y = i\big(|g\rangle\langle e| - |e\rangle\langle g|\big)$ and $\sigma_z = |e\rangle\langle e| - |g\rangle\langle g|$. The first two Pauli matrices define the atomic lowering and rising operators

$$\sigma_\pm = \frac{1}{2}(\sigma_x \pm i\sigma_y), \tag{3.2}$$

with a representation $\sigma_+ = |e\rangle\langle g|$ and $\sigma_- = \sigma_+^\dagger = |g\rangle\langle e|$ in the atomic basis.

The free Hamiltonian of the atom is

$$H_A = \frac{\omega_A}{2}\sigma_z. \tag{3.3}$$

3.2.1 Atom-Field Interactions

The Hamiltonian describing the interaction between an atom and an external field $\mathbf{E}(t)$ in the Coulomb gauge and dipole approximation is

$$H = H_0 - \mathbf{d} \cdot \mathbf{E}(t), \tag{3.4}$$

where H_0 is the free Hamiltonian of the field and $\mathbf{d}$ is the dipole moment operator. The dipole moment is completely non-diagonal in the atomic basis and may be written as $\mathbf{d} = \mathbf{d}_{eg}(\sigma_+ + \sigma_-)$ where $\mathbf{d}_{eg} = \langle e| \mathbf{d} |g\rangle$ can be assumed to be real without loss of generality.

Atom Interacting With a Classical Field

We consider the driving field to be an external perturbation. In this case it is sufficient to treat the driving field as a classical driving field

$$\mathbf{E}_C(t) = \mathcal{E} \cos \omega_L t, \tag{3.5}$$

where ω_L is the frequency of the field. The amplitude of the field $\mathcal{E}$ is assumed to vary so little in time that it is approximated to be time independent.
Defining the Rabi frequency as $\Omega = -\mathbf{d}_{eg} \cdot \mathcal{E}$ we obtain the interaction Hamiltonian

$$H_{I,C} = \mathbf{d} \cdot \mathbf{E}_C(t) = \Omega \, \sigma_x \cos \omega_L t. \tag{3.6}$$

In the near resonant case $|\omega_A - \omega_L| \ll \omega_A$ the expansion of this Hamiltonian contains terms that are negligibly small [27]. The rotating wave approximation (RWA) drops these terms giving

$$H_{I,C} = \frac{\Omega}{2}(\sigma_+ e^{-i\omega_L t} + \sigma_- e^{i\omega_L t}). \tag{3.7}$$

The rotating wave approximation is violated when the interaction between the two-state system and the driving field is strong compared to the interaction between the

two-state system and the environment (see, e.g., Ref. [1]). A study of the effect of a strong driving field on the two-state system requires a different approach than the TCL2 method we employ in this thesis. Namely, to generalize the master equation to be valid for strong periodic driving fields one has to use, e.g., the Floquet theorem. However, such treatment of the dynamics of the system leads to a Markovian master equation. Since we are interested in the non-Markovian effects, we will restrict this study to the case when the interaction of the system with the laser is not stronger than the interaction with the environment and use the TCL2 method to derive the master equation.

Atom Interacting With the Environment

The environment is a quantum multimode field in a thermal state. Following the general theory of quantization of the electromagnetic field (see, e.g., Ref. [32]) we model the field as a chain of infinitely many quantum harmonic oscillators with the energy of the kth field mode corresponding to the frequency of the kth oscillator, ω_k. The free Hamiltonian of the field is

$$H_F = \sum_k \omega_k a_k^\dagger a_k. \tag{3.8}$$

The quantized electric field is given by

$$\mathbf{E}_F = \sum_k \mathcal{E}_k (a_k + a_k^\dagger), \tag{3.9}$$

where a_k and $a_k^\dagger$ are respectively the multimode annihilation and creation operators with commutation relations

$$[a_k, a_{k'}] = 0 = [a_k^\dagger, a_{k'}^\dagger], \qquad [a_k, a_{k'}^\dagger] = \delta_{kk'}, \tag{3.10}$$

and $a_k^\dagger a_k$ is the number operator for the kth mode.

Defining the coupling between the atom and the kth field mode as $g_k = -\mathbf{d}_{eg} \cdot \mathcal{E}_k$

we obtain

$$H_{I,F} = \sum_k g_k \sigma_x (a_k + a_k^\dagger). \tag{3.11}$$

The expansion contains terms that describe processes in which a photon and an excitation of the atom are simultaneously created or destroyed. These energy non-conserving terms are neglected in the second RWA, giving

$$H_{I,F} = \sum_k g_k (\sigma_+ a_k + \sigma_- a_k^\dagger). \tag{3.12}$$

3.2.2 The Rotating Frame

To simplify the calculation we perform a change of frame. The unitary transformation to a frame rotating at the laser frequency is described by the operator

$$U(t) = e^{-i\omega_L t \sigma_z/2}. \tag{3.13}$$

The new Hamiltonian obtained in a time dependent unitary transformation takes the general form

$$H' = U^\dagger(t) H U(t) - i U^\dagger(t) \frac{dU(t)}{dt}. \tag{3.14}$$

Inserting $H = H_A + H_F + H_{I,F} + H_{I,C}$ we obtain after some basic calculations the rotating total Hamiltonian

$$H' = \frac{1}{2}(\Delta\sigma_z + \Omega\sigma_x) + \sum_k [\omega_k a_k^\dagger a_k + g_k (e^{i\omega_L t}\sigma_+ a_k + e^{-i\omega_L t}\sigma_- a_k^\dagger)], \tag{3.15}$$

where the detuning between the atom and the laser has been defined as

$$\Delta = \omega_A - \omega_L. \tag{3.16}$$

The derivation of the rotating microscopic Hamiltonian (3.15) serves as the starting point for the next section, in which the master equation will be derived.

3.3 Master Equation for the Driven Two State System

We decompose the microscopic rotating Hamiltonian H' according to Eq. (2.20), i.e., in terms of the free Hamiltonians of the system and the environment, H_S and H_E respectively, and the interaction Hamiltonian H_I:

$$H_S = \frac{1}{2}(\Delta\sigma_z + \Omega\sigma_x), \tag{3.17}$$

$$H_E = \sum_k \omega_k a_k^\dagger a_k, \tag{3.18}$$

$$H_I = \sum_k g_k(e^{i\omega_L t}\sigma_+ a_k + e^{-i\omega_L t}\sigma_- a_k^\dagger). \tag{3.19}$$

The interaction Hamiltonian is further decomposed into a sum of tensor products of operators belonging to the Hilbert spaces of the system and of the environment according to $H_I = \sum_i S_i \otimes E_i$, $S_i \in \mathcal{H}_S$, $E_i \in \mathcal{H}_E$ and $i = 1, 2$. Specifically

$$S_1 = e^{i\omega_L t}\sigma_+, \quad S_2 = S_1^\dagger, \tag{3.20}$$

$$E_1 = \sum_k g_k a_k, \quad E_2 = E_1^\dagger. \tag{3.21}$$

The eigenvalues and the corresponding eigenvectors of the system Hamiltonian H_S are

$$\begin{aligned} \epsilon_+ &= \frac{\omega}{2}, \quad |\psi_+\rangle = \frac{1}{\sqrt{2\omega}}\big(\sqrt{\omega+\Delta}\,|e\rangle + \sqrt{\omega-\Delta}\,|g\rangle\big), \\ \epsilon_- &= -\frac{\omega}{2}, \quad |\psi_-\rangle = \frac{1}{\sqrt{2\omega}}\big(-\sqrt{\omega-\Delta}\,|e\rangle + \sqrt{\omega+\Delta}\,|g\rangle\big), \end{aligned} \tag{3.22}$$

where we have defined

$$\omega = \sqrt{\Delta^2 + \Omega^2}. \tag{3.23}$$

The eigenstates include the effect of the driving field, and in the limit of no driving, $\Omega \to 0$, the eigenstates approach the atomic states, $|\psi_+\rangle \to |e\rangle$ and $|\psi_-\rangle \to |g\rangle$. Another interesting limit for the eigenstates appears in the case of exact resonance.

In that case $|\psi_+\rangle_{\Delta=0} = \frac{1}{\sqrt{2}}(|e\rangle + |g\rangle)\rangle$ and $|\psi_-\rangle_{\Delta=0} = \frac{1}{\sqrt{2}}(|g\rangle - |e\rangle)$, i.e. the population is equally distributed between the ground state and the excited state of the atom. The eigenvectors are used to calculate the eigenoperators of S_1 and S_2 in the atomic basis. These are

$$\begin{aligned} S_1(\omega) &= e^{i\omega_L t} C_- A, \quad & S_2(\omega) &= e^{-i\omega_L t} C_+ A, \\ S_1(-\omega) &= e^{i\omega_L t} C_+ A^\dagger, \quad & S_2(-\omega) &= e^{-i\omega_L t} C_- A^\dagger, \\ S_1(0) &= e^{i\omega_L t} C_0 B, \quad & S_2(0) &= e^{-i\omega_L t} C_0 B, \end{aligned} \tag{3.24}$$

where the auxiliary operators A and B are given by

$$A = -\Omega\sigma_z + (\Delta - \omega)\sigma_+ + (\Delta + \omega)\sigma_-, \tag{3.25}$$

$$B = \Delta\sigma_z + \Omega(\sigma_+ + \sigma_-), \tag{3.26}$$

and coefficients $C_\pm$ and C_0 are

$$C_\pm = \frac{\Delta \pm \omega}{4\omega^2}, \quad C_0 = \frac{\Omega}{2\omega^2}. \tag{3.27}$$

3.3.1 Eigenbasis of the System

The equations simplify greatly if we change the basis of $\mathcal{H}_S$ from the atomic basis $\{|e\rangle, |g\rangle\}$ to the eigenbasis of the system $\{|\psi_+\rangle, |\psi_-\rangle\}$. The eigenstates form the so called *preferred basis* of the system in the weak coupling regime. The preferred states are states that are most robust under the effect of decoherence. The preferred basis are, as implied by their name, the optimal choice of basis for the study of decoherence [33]. Furthermore, the eigenbasis consists of the stationary states of the system when the interaction with the environment is neglected and therefore the Rabi oscillations are not present in the eigenbasis. We will see that the non-Markovian oscillations are negligible compared to the Rabi oscillations and therefore the non-Markovian effects are more visible in the eigenbasis than in the atomic basis. In the eigenbasis the Hamiltonian of the system is diagonal, $H_S = diag(\epsilon_+, \epsilon_-)$, and

the auxiliary operators given in Eq. (3.25) simplify to

$$A = 2\omega\bar{\sigma}_-, \quad A^\dagger = 2\omega\bar{\sigma}_+, \quad B = \omega\bar{\sigma}_z, \tag{3.28}$$

where

$$\begin{aligned} \bar{\sigma}_+ &= |\psi_+\rangle\langle\psi_-|, \\ \bar{\sigma}_- &= \bar{\sigma}_+^\dagger, \qquad (3.29) \\ \bar{\sigma}_z &= |\psi_+\rangle\langle\psi_+| - |\psi_-\rangle\langle\psi_-| \qquad (3.30) \end{aligned}$$

are the spin operators in the eigenbasis. The transformation from the atomic basis to the eigenbasis is fully analogous to the transformation to the dressed state basis in the Jaynes-Cummings model.

We now carry out the usual transformation to the interaction picture using equations (2.31) and (2.33). The interaction Hamiltonian in the interaction picture becomes time dependent,

$$\tilde{H}_I(t) = \sum_{i=1,2} \tilde{S}_i(t) \otimes \tilde{E}_i(t), \tag{3.31}$$

with

$$\begin{aligned} \tilde{S}_1(t) &= \frac{e^{i\omega_L t}}{2\omega}[e^{-i\omega t}(\Delta-\omega)\bar{\sigma}_- + e^{i\omega t}(\Delta+\omega)\bar{\sigma}_- + \Omega\bar{\sigma}_z], \\ \tilde{S}_2(t) &= \frac{e^{-i\omega_L t}}{2\omega}[e^{-i\omega t}(\Delta+\omega)\bar{\sigma}_- + e^{i\omega t}(\Delta-\omega)\bar{\sigma}_+ + \Omega\bar{\sigma}_z], \qquad (3.32) \\ \tilde{E}_1(t) &= \sum_k g_k a_k e^{-i\omega_k t}, \\ \tilde{E}_2(t) &= \sum_k g_k^* a_k^\dagger e^{i\omega_k t}. \qquad (3.33) \end{aligned}$$

Inserting the interaction Hamiltonian into the TCL2 (Redfield) master equation of Eq. (2.70) we obtain

$$\begin{aligned} \frac{d}{dt}\tilde{\rho}_S(t) &= \sum_{i,j=1,2}\int_0^t d\tau \left[\tilde{S}_j(t-\tau)\tilde{\rho}_S(t)\tilde{S}_i(t) - \tilde{S}_i(t)\tilde{S}_j(t-\tau)\tilde{\rho}_S(t)\right] \times \\ & \qquad tr_E\{\tilde{E}_i(t)\tilde{E}_j(t-\tau)\rho_E\} + H.c. \qquad (3.34) \end{aligned}$$

where we have set the initial time $t_0 = 0$.

3.3.2 The Environment

To continue with the study of the system dynamics we now need to specify the environment in more detail. An environment of infinitely many quantum harmonic oscillators in a thermal equilibrium in temperature T is described by a density matrix

$$\rho_E = \frac{1}{Z} \exp\{ -\sum_n \frac{\omega_n a_n^\dagger a_n}{k_B T} \}, \tag{3.35}$$

where Z is the partition function and k_B is the Boltzmann constant. For such a state we obtain the following expectation values for the field operators:

$$\begin{aligned} \langle a_k a_{k'} \rangle &\equiv tr\{a_k a_{k'} \rho_E\} = 0, & \langle a_{k'} a_k \rangle &= 0, \\ \langle a_k^\dagger a_{k'} \rangle &= \delta_{k,k'} N(\omega_k), & \langle a_k a_{k'}^\dagger \rangle &= \delta_{k,k'}(1 + N(\omega_k)), \end{aligned}$$

where

$$N(\omega_k) = \frac{1}{e^{-\omega_k / k_B T} - 1} \tag{3.36}$$

is the average number of photons in the kth mode at temperature T. In the zero temperature case $N(\omega_k) = 0$.

This auxiliary result is used to calculate the reservoir correlation functions

$$\begin{aligned} tr_E\{\tilde{E}_1(\tau)\tilde{E}_1(0)\rho_E\} &= 0, \\ tr_E\{\tilde{E}_1(\tau)\tilde{E}_2(0)\rho_E\} &= \sum_k |g_k|^2 e^{-i\omega_k \tau} \big(N(\omega_k) + 1\big), \\ tr_E\{\tilde{E}_2(\tau)\tilde{E}_1(0)\rho_E\} &= \sum_k |g_k|^2 e^{i\omega_k \tau} N(\omega_k), \\ tr_E\{\tilde{E}_2(\tau)\tilde{E}_2(0)\rho_E\} &= 0. \end{aligned} \tag{3.37}$$

For convenience we consider the modes of the electromagnetic field in the continuum limit, i.e. $\sum_k |g_k|^2 \to \int d\omega' J(\omega')$. $J(\omega')$ is the spectral density defined as the product

$d(\omega)|g_k|^2$, where $d(\omega)$ is the density of states and g_k describes the coupling between the kth field mode and the atom.

The properties of the environment at $T = 0$ allow to recast Eq. (3.34) in the following form:

$$\begin{aligned}\frac{d}{dt}\tilde{\rho}_S(t) &= \int_0^t d\tau \int_0^\infty d\omega'\, J(\omega') e^{-i\omega'\tau} \left[\tilde{S}_2(t-\tau)\tilde{\rho}_S(t)\tilde{S}_1(t) - \tilde{S}_1(t)\tilde{S}_2(t-\tau)\tilde{\rho}_S(t)\right] \\ &\quad + H.c. \end{aligned} \tag{3.38}$$

3.3.3 Master Equation in the Secular Approximation

The typical timescale of the system is $\tau_S = \omega^{-1}$. If the relaxation time is very large compared to the typical timescale of the system, $\tau_R \gg \tau_S$, oscillating terms like $e^{\pm i\omega t}$ and $e^{\pm 2i\omega t}$ may be neglected since rapid oscillations average out to zero on the timescale of the relaxation process. This coarse graining constitutes the secular approximation.

We assume initially that the secular approximation can be performed. This assumption leads to a Lindblad type master equation which, when transformed back to the Schrödinger picture reads

$$\begin{aligned}\frac{d}{dt}\rho_S(t) &= -i[H_S + H_{LS}, \rho_S(t)] \\ &+ \gamma_+(t)\big(\bar{\sigma}_-\rho_S(t)\bar{\sigma}_+ - \frac{1}{2}\{\bar{\sigma}_+\bar{\sigma}_-, \rho_S(t)\}\big) \\ &+ \gamma_-(t)\big(\bar{\sigma}_+\rho_S(t)\bar{\sigma}_- - \frac{1}{2}\{\bar{\sigma}_-\bar{\sigma}_+, \rho_S(t)\}\big) \\ &+ \gamma_0(t)\big(\bar{\sigma}_z\rho_S(t)\bar{\sigma}_z - \frac{1}{2}\{\bar{\sigma}_z\bar{\sigma}_z, \rho_S(t)\}\big), \end{aligned} \tag{3.39}$$

where the Lamb shift Hamiltonian is

$$H_{LS} = \lambda_+(t)\bar{\sigma}_-\bar{\sigma}_+ + \lambda_-(t)\bar{\sigma}_+\bar{\sigma}_- + \lambda_0(t)\bar{\sigma}_z^2, \tag{3.40}$$

and the decomposition of the Fourier transform of the reservoir correlation function into real and imaginary parts gives the decay rates

$$\gamma_{\pm}(t) = \Big[\frac{\Delta \pm \omega}{2\omega}\Big]^2 \int_0^t d\tau \int_0^\infty d\omega'\, 2J(\omega')\cos(\omega_L - \omega' \pm \omega)\tau, \tag{3.41}$$

$$\lambda_{\pm}(t) = \Big[\frac{\Delta \pm \omega}{2\omega}\Big]^2 \int_0^t d\tau \int_0^\infty d\omega'\, J(\omega')\sin(\omega_L - \omega' \pm \omega)\tau, \tag{3.42}$$

$$\gamma_0(t) = \Big[\frac{\Omega}{2\omega}\Big]^2 \int_0^t d\tau \int_0^\infty d\omega'\, 2J(\omega')\cos(\omega_L - \omega')\tau, \tag{3.43}$$

$$\lambda_0(t) = \Big[\frac{\Omega}{2\omega}\Big]^2 \int_0^t d\tau \int_0^\infty d\omega'\, J(\omega')\sin(\omega_L - \omega')\tau. \tag{3.44}$$

In terms of the quantum jump description briefly recalled in Sec. 2.2.3, Eq. (3.39) tells us that the dissipative dynamics can be described in terms of three different decay channels. Two channels are associated with the jump operators $\bar{\sigma}_{+/-}$, inducing jumps up/down between the eigenstates at rates $\gamma_{+/-}(t)$. The third channel is associated with the jump operator σ_z, inducing phase-flips at a rate $\gamma_0(t)$. The three quantum jump channels are in a Lindblad type form, but with the important difference of having time dependent coefficients $\gamma(t)$. The up and down jumps cause both a change in the eigenstate populations and a change in the coherences, while the phase flips only affect the coherences in the eigenbasis.

3.4 The Decay Rates

In the derivation of the microscopic Hamiltonian we assumed that the system is near resonant, $|\Delta| \ll \omega_A$. Furthermore, in typical optical situations $\Omega \ll \omega_L, \omega_A$ and indeed both of these conditions are implicitly included in the two-level description of the atom. Therefore $\omega = \sqrt{\Delta^2 + \Omega^2} \ll \omega_L$ so we can replace the argument of the trigonometric functions appearing in Eqs. (3.41)-(3.44) with $\omega_L - \omega'$. In this

approximation the decay rates simplify as follows:

$$\gamma_{\pm}(t) = \left[\frac{\Delta \pm \omega}{2\omega}\right]^2 \gamma(t), \qquad \gamma_0(t) = \left[\frac{\Omega}{2\omega}\right]^2 \gamma(t), \tag{3.45}$$

$$\lambda_{\pm}(t) = \left[\frac{\Delta \pm \omega}{2\omega}\right]^2 \lambda(t), \qquad \lambda_0(t) = \left[\frac{\Omega}{2\omega}\right]^2 \lambda(t), \tag{3.46}$$

where

$$\gamma(t) = 2\int_0^t d\tau \int_0^\infty d\omega'\, J(\omega') \cos[(\omega_L - \omega')\tau], \tag{3.47}$$

$$\lambda(t) = \int_0^t d\tau \int_0^\infty d\omega'\, J(\omega') \sin[(\omega_L - \omega')\tau]. \tag{3.48}$$

The quantities $\gamma(t)$ ad $\lambda(t)$ fully determine the dynamics of the decay rates; the decay rates for each channel, given by Eqs. (3.45) and (3.46) have the same dynamics but with different weights.

To find a closed analytical expression for the decay rates we must define the spectral density that describes the properties of the environment. In the following we consider two different spectral densities, corresponding to two different types of environments.

The Ohmic Reservoir

We begin by considering the Ohmic spectral density, which is linear in ω in the optical regime, $J(\omega) \sim \omega$. Physically, spectral densities must fall off in the limit of large frequencies and a cut-off function has to be included in the definition of the Ohmic spectral density in order to avoid divergencies. We consider an exponentially decaying cut-off function. The Ohmic spectral density then reads as follows

$$J(\omega) = \frac{\alpha}{2}\omega e^{-\omega/\omega_C}, \tag{3.49}$$

where ω_C is the cut-off frequency and α is the coupling constant assumed to be much smaller than unity in the weak-coupling regime.

The structure of the spectral density depends on the value of the cut-off frequency ω_C, which determines the position of the peak of the distribution and gives a rough

approximation for the width of the distribution. Values of $\omega_C \lesssim \omega_A$ are typically associated to more structured reservoirs. The reservoir correlation time is defined as the inverse of the cut-off frequency $\tau_C = \omega_C^{-1}$ and hence a structured reservoir implies a long reservoir correlation time.

For the Ohmic spectral density the decay rates are

$$\begin{aligned}
\gamma_O(t) &= \frac{\alpha\,\omega_C}{1+t^2\omega_C^2}\big(t\omega_C\cos\omega_L t - \sin\omega_L t\big) \\
&\quad + \frac{\alpha}{2}\,\omega_L\,e^{-\omega_L/\omega_C}\Big[\pi - i(\mathrm{Ci}\,z - \mathrm{Ci}\,z^*) + \mathrm{Si}\,z + \mathrm{Si},z^*\Big], \qquad (3.50)\\
\lambda_O(t) &= \frac{\alpha}{2}\frac{\omega_C}{1+t^2\omega_C^2}\big(\cos\omega_L t + t\omega_C\sin\omega_L t - 1 - t^2\omega_C^2\big) \\
&\quad + \frac{\alpha}{2}\,\omega_L\,e^{-\omega_L/\omega_c}\Big[2\big(\mathrm{Chi}\,\frac{\omega_L}{\omega_c} + \mathrm{Shi}\,\frac{\omega_L}{\omega_c}\big) - \mathrm{Ci}\,z - \mathrm{Ci}\,z^* + i\big(\mathrm{Si}\,z - \mathrm{Si}\,z^*\big)\Big], \qquad (3.51)
\end{aligned}$$

where the variable $z = \omega_L(t - \frac{i}{\omega_c})$ and the sine, cosine, hyperbolic sine and hyperbolic cosine integrals are defined as

$$\begin{aligned}
\mathrm{Si}\,z &= \int_0^z dt\,\frac{\sin t}{t}, \quad \mathrm{Ci}\,z = \gamma_{EM} + \ln z + \int_0^z dt\,\frac{\cos t - 1}{t}, \\
\mathrm{Shi}\,z &= \int_0^z dt\,\frac{\sinh t}{t}, \quad \mathrm{Chi}\,z = \gamma_{EM} + \ln z + \int_0^z dt\,\frac{\cosh t - 1}{t},
\end{aligned}$$

respectively, and $\gamma_{ME} \approx 0.577$ is the Euler-Mascheroni constant.

The stationary values of the decay rates are given by

$$\begin{aligned}
\gamma_O &= \lim_{t\to\infty}\gamma(t) = \alpha\,\pi\,\omega_L\,e^{-\omega_L/\omega_c}, \qquad (3.52)\\
\lambda_O &= \lim_{t\to\infty}\gamma(t) = \frac{\alpha}{2}\,\omega_L\,e^{-\omega_L/\omega_c}\,\mathrm{Ei}\left[\frac{\omega_L}{\omega_c}\right] - \omega_C, \qquad (3.53)
\end{aligned}$$

where the exponential integral is defined as

$$\mathrm{Ei}\,z = \int_{-\infty}^z dt\,\frac{e^t}{t}. \qquad (3.54)$$

The Lorenzian Reservoir

The second type of spectral density considered is the Lorentzian spectral density

$$J(\omega) = \frac{\alpha}{2\pi} \frac{\Lambda^2}{(\omega - \omega_0)^2 + \Lambda^2}, \tag{3.55}$$

where α is the coupling constant,[1] ω_0 specifies the location of the peak of the distribution and Λ defines the width of the distribution. This type of environment describes, e.g., the quantized electromagnetic field inside a lossy resonator, where ω_0, the mode supported by the cavity, is almost resonant with the atom.

Physically the width of the distribution gives the cavity quality factor. The optimal case $\Lambda \to 0$, corresponds to an ideal lossless cavity. When the cavity losses are dominant, $\Lambda \to \infty$ and the spectral density is practically flat, approaching a Markovian environment. The inverse of the width defines the reservoir correlation time $\tau_C = \Lambda^{-1}$. As we mentioned in the case of the Ohmic spectral density, a structured reservoir has a long reservoir correlation time.

For the Lorentzian spectral density the decay rates take simple analytical forms:

$$\begin{aligned} \gamma_L(t) &= \frac{\alpha}{2}\Big[\frac{\Lambda^2}{\delta^2 + \Lambda^2} + e^{-\Lambda t}\frac{\delta \sin \delta t - \Lambda \cos \delta t}{\delta^2 + \Lambda^2}\Big], \\ \lambda_L(t) &= \frac{\alpha}{2}\Big[-\frac{\Lambda\delta}{\delta^2 + \Lambda^2} + e^{-\Lambda t}\frac{\delta \cos \delta t + \Lambda \sin \delta t}{\delta^2 + \Lambda^2}\Big], \end{aligned} \tag{3.56}$$

where we defined $\delta \equiv \omega_0 - \omega_L$ to be the detuning between the peak of the distribution and the frequency of the laser.

The stationary values of the decay rates are

$$\begin{aligned} \gamma_L &= \frac{\alpha}{2}\frac{\Lambda^2}{\delta^2 + \Lambda^2}, \\ \lambda_L &= -\frac{\alpha}{2}\frac{\Lambda\delta}{\delta^2 + \Lambda^2}. \end{aligned} \tag{3.57}$$

[1]Note that now α has the dimension of frequency and the weak coupling approximation is valid when α is smaller than all other relevant frequencies.

Dynamics of the Decay Rates

Figure 3.1 shows the dynamic of the Ohmic decay rate $\gamma_O(t)$ for three different values of $\frac{\omega_C}{\omega_A}$. It is evident that the amount of detuning between the cut-off frequency and the Bohr frequency essentially determines the dynamics of the decay rates. For small values of detuning $\Delta = \omega_A - \omega_L$ the decay rate converges rapidly towards its stationary value, whereas for large detunings the convergence is slower, and the decay rate exhibits oscillations around its stationary value. When the Bohr frequency ω_A is detuned considerably from the cut-off frequency ω_C the decay rate oscillates, taking temporarily negative values. Furthermore, as the value of the detuning Δ increases, the effective coupling between the two-state system and its environment decreases. This leads to a decreased magnitude of the decay rates.

Figure 3.2 shows the dynamic of the Lorentzian decay rate $\gamma_L(t)$ for a constant width Λ and three different values of the detuning parameter $\delta = \omega_0 - \omega_L$. Similarly to the Ohmic decay rates, it is this detuning between the center of the distribution and the Bohr frequency that determines the presence or the absence of the oscillations around the stationary value of the decay rate. The more detuned the system is, the larger are the oscillations of the decay rate around its stationary value. Also in this case when the detuning is sufficiently large, the decay rate temporarily attains negative values and an increase in the detuning δ causes a decrease in the magnitude of the decay rate.

For the Lorentzian decay rates the convergence time is determined by the width of the distribution Λ. This is evident in figure 3.2, where Λ is constant for all three cases and all curves converge to their stationary value at the same time, regardless of the amount of oscillations around the stationary value. This property is not a characteristic of the Ohmic decay rates because the width and the detuning of the Ohmic rates are determined by the same parameter. Therefore the cut-off frequency of the Ohmic spectral density determines both the reservoir correlation time and

the amplitude of the oscillations of the decay rate around its stationary value. This means that the Lorentzian reservoir is more tunable than the Ohmic reservoir; the reservoir correlation time, i.e., the time it takes for the decay rate to reach its stationary value, can be manipulated by tuning the width of the Lorentzian and the appearance and amplitude of oscillations around the stationary value by choosing the detuning appropriately. However, when the reservoir correlation time is increased, the value of the detuning has to be likewise increased to obtain large deviations of the rates from their stationary values. In particular, the Lorentzian decay rate attains temporarily negative values whenever $\delta \gtrsim 3.5\Lambda$ for any value of Λ.
It is worth noting that for both types of reservoir the case of $\Delta \neq 0$ exhibits the same qualitative behavior as the case of $\Delta = 0$.

3.5 Decay Rates and the Reservoir Memory

Recall that the Markovian approximation amounts at replacing the upper limit of integration in Eqs. (3.47) and (3.48) with infinity. This is equivalent to replacing the time-dependent decay rates by their stationary values. When $\gamma(t) \approx \gamma$, the dynamics of the system is essentially Markovian. Therefore when the decay rates deviate strongly from their stationary values, the non-Markovian effects are most evident in the dynamics. Furthermore, the slower is the convergence of the decay rate to its stationary value, the longer is the timescale of the non-Markovian effects. Evidently the decay rates give a good indication of the qualitative behavior of the non-Markovian effects.
The periods when $\gamma(t) < 0$ have a dramatic effect on the dynamics of the system. For example, from the point of view of the Markovian quantum jump method described in Sec. 2.2.3 negative decay rates imply negative probabilities for the occurrence of the jumps, indicating that the Markovian description of quantum jump

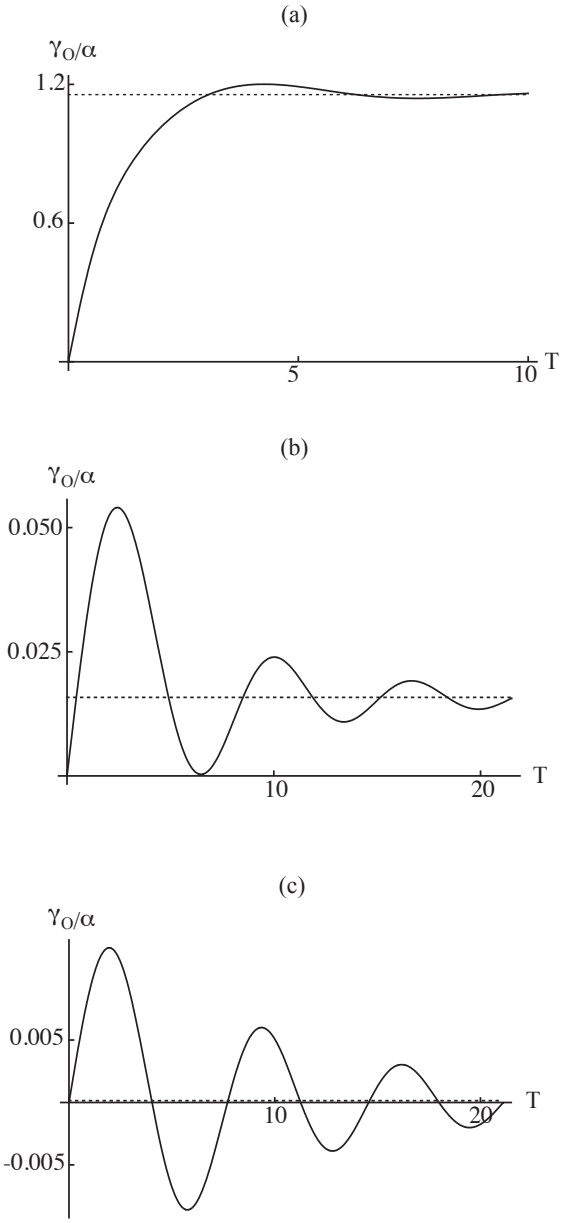

Figure 3.1: The Ohmic decay rate $\frac{\gamma_O(T)}{\alpha}$ as a function of $T = \omega_A t$ for $\Delta = 0$ and (a) $\omega_C = \omega_A$, (b) $\omega_C = 0.2\omega_A$ and (c) $\omega_C = 0.1\omega_A$. In each figure the dashed line denotes the stationary value of the decay rate.

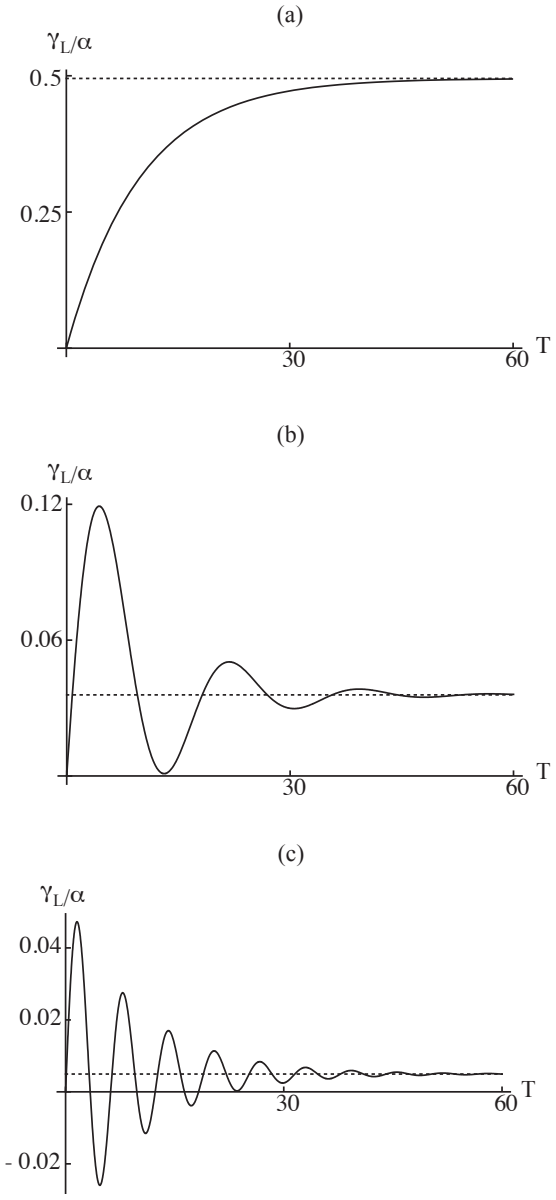

Figure 3.2: The Lorentzian decay rate $\frac{\gamma_L(T)}{\alpha}$ as a function of $T = \omega_A t$ for $\Delta = 0$, $\Lambda = 0.1\,\omega_A$ and (a) $\delta = 0.1\omega_A$, (b) $\delta = 0.35\omega_A$ and (c) $\delta = \omega_A$. In each figure the dashed line denotes the stationary value of the decay rate.

processes breaks down. Indeed, when the decay rates become negative a more general description for the jump processes, namely the non-Markovian quantum jump (NMQJ) method has to be considered [5, 6].

According to the NMQJ approach, when the decay rate of a jump channel becomes negative, the direction of the jump is reversed and the probability for the jump to happen is proportional to the target state, rather than to the present state. This description explains how a non-local master equation, such as the TCL2 master equation that we consider in this thesis, can contain memory effects and in particular how the reservoir memory effects are connected to the time-dependent decay rates.

When the direction of the jumps is reversed due to the negative values of the decay rates, the flow of information and energy is reversed, i.e., they flow from the environment to the system. In particular this means that the system can recohere, i.e., regain coherence and previously lost superposition states of the system and be reconstructed.

3.6 Full Non-Markovian Master Equation

The secular approximation is generally useful when one is interested in the relaxation process of an open quantum system, i.e., in the time evolution for long timescales. The situation changes dramatically when we are interested in the non-Markovian dynamics, i.e., in the dynamics on the timescale of the reservoir correlation time.

The fact that the reservoir correlation time is extremely short in comparison with the relaxation time is utilized in the Markovian approximation. Markovian and secular approximation often go hand-in-hand, both being coarse grainings on the timescale of the relaxation.

However, the effect of the rapidly oscillating terms is far from trivial when we wish

to study the non-Markovian timescale. A secular approximation from the point of view of the non-Markovian dynamics would require the typical timescale of the system to be much smaller than the non-Markovian timescale.

Recall that the typical timescale is $\tau_S = \omega^{-1} = (\Delta^2 + \Omega^2)^{-1/2}$ and that both the detuning and the driving are assumed to be small compared to the atomic frequency. This leads to a remarkably long typical timescale of the system, in particular in comparison to the small non-Markovian timescale τ_C. Therefore the secular approximation is very non-trivial in the study of non-Markovian dynamics in this system. For this reason we also consider the full non-Markovian master equation, i.e., the master equation where neither the secular nor the Markovian approximations have been made. We start again from Eq. (3.38) and after some algebra we obtain the following master equation:

$$\begin{aligned}
\frac{d}{dt}\rho_S(t) &= -i[H_S, \rho_S(t)] + \mathcal{D}[\rho_S(t)] \\
&\quad + \gamma(t)\,\frac{\Omega}{4\omega^2}\Big[(\Delta-\omega)\big(\bar{\sigma}_+\rho_S(t)\bar{\sigma}_z + \bar{\sigma}_z\rho_S(t)\bar{\sigma}_-\big) \\
&\quad + (\Delta+\omega)\big(\bar{\sigma}_-\rho_S(t)\bar{\sigma}_z + \bar{\sigma}_z\rho_S(t)\bar{\sigma}_+\big) \\
&\quad - \Omega\big(\bar{\sigma}_+\rho_S(t)\bar{\sigma}_+ + \bar{\sigma}_-\rho_S(t)\bar{\sigma}_-\big)\Big] \\
&\quad + \frac{\Omega}{2\omega}\Big(\frac{\gamma(t)}{2}\{\bar{\sigma}_x, \rho_S(t)\} + i\lambda(t)[\bar{\sigma}_x, \rho_S(t)]\Big),
\end{aligned} \tag{3.58}$$

where the dissipator $\mathcal{D}[\rho_S(t)]$ describes the non-unitary evolution in Eq. (3.39). We have neglected the Lamb shift since it does not affect the dynamics in a qualitative way. In the secular approximation only the real part of the Fourier transform of the reservoir correlation, namely $\gamma(t)$, appears in the master equation. However, the full master equation also includes the imaginary part of the Fourier transform of the reservoir correlation function, $\lambda(t)$.

The full non-Markovian master equation contains some very non-standard terms that are not easily interpreted in the context of quantum jumps, because they are not in the Lindblad form.

In the next chapter we will study the system dynamics using both the secular approximated master equation, given by Eq, (3.39), and the full master equation, given by Eq. (3.58). In this way we will be able to understand if, and under which conditions, the non-secular terms are negligible in the description of the system dynamics.

3.7 Comparison to Literature

Most of the existing literature on driven two-level atoms in a zero-T reservoir (e.g., Refs. [1, 27, 34, 35]) use the following master equation in the rotating frame:

$$\frac{d\rho_S(t)}{dt} = -i[H_S, \rho_S(t)] + \gamma\Big[\sigma_-\rho_S(t)\sigma_+ - \frac{1}{2}\{\sigma_+\sigma_-, \rho_S(t)\}\Big], \tag{3.59}$$

where $H_S = \frac{1}{2}(\Omega\sigma_x + \Delta\sigma_z)$ and the operators are in the atomic basis. A master equation of this form assumes that the effect of the driving field and the effect of the environment are independent events, hence dissipative processes only happen via the jump down-channel, described by operator σ_-. According to Cohen-Tannoudji *et al.* [27], this approximation is valid when $\Omega \ll \omega_A$, which is, indeed, the case in realistic optical situations.

The full master equation (3.58) coincides with Eq. (3.59) in the Markovian limit when $\frac{\Omega}{\Delta} \to 0$. This latter condition implies that $\Omega \ll \omega_A$, but it is a stricter condition: the strength of the driving should be compared to the detuning rather than to the Bohr frequency.

A microscopic derivation closely paralleling our derivation has been carried out by Kowalewska-Kudłaszyk and Tanaś in the Born-Markov approximation using a Lorentzian reservoir [36, 37]. In particular the master equation of Kowalewska-Kudłaszyk and Tanaś contains the same non-standard terms, such as those proportional to $\sigma_x\rho\sigma_\pm$ etc., that we found to appear when the non-secular terms are taken into account. Our master equation (3.58) reduces to the Markovian master equation of Kowalewska-Kudłaszyk and Tanaś for times longer than the reservoir correlation

time. In this sense our master equation is the first non-Markovian generalization of the full equation of motion correctly describing the system dynamics.

Non-Markovian generalizations for the dynamics of the driven two-state systems have been previously considered in the literature. However, such approaches always neglect the non-secular terms. As we will see in the next chapter, the contribution of such terms is non-negligible for both short non-Markovian time scales and long relaxation time scales.

Finlally, we note that Budini considers a phenomenological model of a driven two-level atom in a zero-T reservoir described by the following master equation [38]:

$$\frac{d\rho_S(t)}{dt} = -i[H_S, \rho_S(t)] + \int_0^t d\tau\, K(t-\tau)\big(\sigma_-\rho_S(\tau)\sigma_+ - \frac{1}{2}\{\sigma_+\sigma_-, \rho_S(\tau)\}\big). \quad (3.60)$$

Budini's master equation is a non-local in time extension of the master equation (3.59) equipped with a memory kernel and an integration over the history of the system. Because in the weak coupling limit the time-convolutionless master equation quite accurately coincides with the non-local master equation with a memory kernel, we expect that our master equation (3.58) coincides with Budini's master equation in the weak coupling limit when $\frac{\Omega}{\Delta} \to 0$.

Chapter 4

Dynamics of a Driven Two State System

4.1 Optical Bloch Equations

We study the the dynamics of the driven two-state system using the Bloch vector $\mathbf{R} = (S_x, S_y, S_z)$, where

$$S_x = \langle \sigma_x \rangle, \quad S_y = \langle \sigma_y \rangle, \quad \text{and} \quad S_z = \langle \sigma_z \rangle. \tag{4.1}$$

A 2×2-density matrix is uniquely connected to the Bloch vector through the relation

$$\rho = \frac{1}{2}[\mathbb{I} + \mathbf{R} \cdot \sigma] = \frac{1}{2} \begin{pmatrix} 1 + S_z & S_x - iS_y \\ S_x + iS_y & 1 - S_z \end{pmatrix}, \tag{4.2}$$

where the vector $\sigma = (\sigma_x, \sigma_y, \sigma_z)$ has the Pauli matrices as its components. S_x and S_y are connected to the real and imaginary parts of the coherences of the quantum state while S_z is directly proportional to the occupation probabilities of the quantum state.

A density matrix describes a physical state of a quantum system when $Tr(\rho) = 1$ and $\rho \geq 0$. It is easy to see that the former condition is trivially satisfied for all

Bloch vectors $\mathbf{R}$. The latter property is equivalent to requiring that the eigenvalues of ρ are positive, i.e.,

$$\lambda_\pm = \frac{1}{2}\big[1 \pm |\mathbf{R}|\big] \geq 0 \quad \Rightarrow \quad |\mathbf{R}| \leq 1. \tag{4.3}$$

This condition implies that all Bloch vectors corresponding to quantum physical states are confined in a three dimensional unit ball, the Bloch ball. The position of the Bloch vector in the Bloch ball contains some information about the purity of the quantum state: All Bloch vectors of pure states have a unit norm, $|\mathbf{R}| = 1$, and they cover the surface of the Bloch ball, i.e., the Bloch sphere. All mixed states are characterized by $|\mathbf{R}| < 1$ and they occupy the space inside the Bloch sphere.

The two measures of mixedness of a state that we will use in the following, namely the purity and the von Neumann entropy, take a simple form in the Bloch vector representation, namely

$$\xi(\rho) = \frac{1}{2}\big[1 + |\mathbf{R}|^2\big], \tag{4.4}$$

$$S(\rho) = \frac{1}{2}\big[\log 4 - (1 + |\mathbf{R}|)\log(1 + |\mathbf{R}|) - (1 - |\mathbf{R}|)\log(1 - |\mathbf{R}|)\big], \tag{4.5}$$

and we see that both quantities only depend on the norm of the Bloch vector. We also see that a maximally mixed state is represented by a null Bloch vector, $\mathbf{R} = (0, 0, 0)$.

The time derivatives of the components of the Bloch vector

$$\frac{d}{dt}\langle\sigma_i\rangle = \mathrm{Tr}\Big[\sigma_i \frac{d\rho}{dt}\Big], \quad i = x, y, z \tag{4.6}$$

are the average values of the Pauli matrices with respect to the time derivative of $\rho(t)$. Therefore any equation of motion for the density matrix can be mapped into a set of equations of motion for the components of the Bloch vector. These equations are called the *optical Bloch equations*, named after a very similar set of equations, derived by Felix Bloch, for the dynamics of a spin interacting with a magnetic field [39].

4.1.1 Properties of Mappings in the Bloch Ball

As discussed in chapter 2, any dynamical mapping $\Phi : \rho \mapsto \Phi(\rho)$ must take elements of $\mathcal{S}(\mathcal{H})$ to elements of $\mathcal{S}(\mathcal{H})$, i.e., if $\rho \geq 0$ and $tr[\rho] = 1$, we must have $\Phi(\rho) \geq 0$ and $tr[\Phi(\rho)] = 1$. This restricts the solutions of the optical Bloch equations to be described by affine transformations

$$\Phi : \mathbf{R} \mapsto \mathbf{R}' = \Lambda\mathbf{R} + \mathbf{r}, \tag{4.7}$$

where Λ represents some deformation of the Bloch vector and $\mathbf{r} = (r_1, r_2, r_3)$ a translation [40, 41]. The deformation matrix can be cast into a diagonal form $\Lambda = \mathrm{diag}(\lambda_1, \lambda_2, \lambda_3)$ and whenever $|\lambda_i| \leq 0, \forall\, i = 1, 2, 3$, the norm of the Bloch vector decreases and the mapping Φ is positive.

The more restrictive requirement of complete positivity is in general harder to quantify but holds for unital maps, i.e., in the case $\mathbf{r} = 0$, when the Bloch inequalities

$$\begin{aligned} \lambda_1 + \lambda_2 - \lambda_3 \leq 1, \qquad & \lambda_1 - \lambda_2 + \lambda_3 \leq 1, \\ -\lambda_1 + \lambda_2 + \lambda_3 \leq 1, \qquad & \lambda_1 - \lambda_2 - \lambda_3 \leq 1 \end{aligned} \tag{4.8}$$

are satisfied.

The Bloch sphere evolves under the mapping (4.7) to an ellipsoid

$$\Phi : S_x^2 + S_y^2 + S_z^2 = 1 \mapsto \left(\frac{S_x - r_1}{\lambda_1}\right)^2 + \left(\frac{S_y - r_2}{\lambda_2}\right)^2 + \left(\frac{S_z - r_3}{\lambda_3}\right)^2 = 1. \tag{4.9}$$

The ellipsoid is, in general, rotated and inverted and is always contained within the Bloch sphere. Non-Markovian dynamics are manifested as oscillations of the Bloch vector, as we will see in a later section.

Generally, the interaction between the two-state system and its environment causes the Bloch vector to shrink due to the irreversible dissipation of energy and information, while the coupling to a driving field causes the Bloch vector to rotate.

These properties of a trace preserving CP mapping have been shown to apply also for

non-Markovian dynamics, in which case the damping matrix is time dependent, i.e., $\lambda_i = \lambda_i(t)$ [42, 43, 44]. It is crucial to stress, however, that in the non-Markovian case complete positivity does not necessarily hold for all values of relevant parameters. It has been shown, e.g., that a phenomenological non-Markovian master equation for a spin-boson model describes the dynamics of the system for moderate and high temperatures, but always violates CP for low temperatures [44].

In the non-Markovian case, however, it is not always possible to find a closed analytical form of the matrix elements of Λ and of the vector $\mathbf{r}$, therefore the conditions for positivity and CP are not easy to derive in the general case. Furthermore, we will see in the following that the solution of the full master equation (3.58) is not described by a unital map, i.e., by a mapping of the form of Eq. (4.7) with $\mathbf{r} = 0$, and the Bloch inequalities of Eq. (4.8) are not the necessary and sufficient conditions for CP.

4.1.2 Dynamics in the Atomic Basis

So far the driven two-state system has been studied in the eigenbasis $\{|\Psi_+\rangle, |\Psi_-\rangle\}$ of the system. In the Bloch vector representation a change to the atomic basis $\{|e\rangle, |g\rangle\}$ has a simple geometrical interpretation. Defining

$$\theta = \arctan\frac{\Omega}{\Delta} \Leftrightarrow \begin{cases} \sin\theta &= \frac{\Omega}{\omega} \\ \cos\theta &= \frac{\Delta}{\omega} \end{cases} \tag{4.10}$$

we find that

$$\begin{aligned} S_x &= -\sin\theta S'_z + \cos\theta S'_x, \\ S_y &= S'_y, \\ S_z &= \cos\theta S'_z + \sin\theta S'_x, \end{aligned} \tag{4.11}$$

where S_i are the components of the Bloch vector in the eigenbasis and S'_i in the atomic basis. Thus a change to the atomic basis from the eigenbasis corresponds to

a rotation of the Bloch vector by an angle θ around the y-axis. We note that for the case of no driving, $\Omega = 0$, the Bloch vectors in the two basis coincide and in the case of exact resonance, $\Delta = 0$, the angle $\theta = \frac{\pi}{2}$ and the Bloch vectors in the two basis are orthogonal.

4.2 Relaxation Dynamics

We begin our analysis by considering the long time scale relaxation dynamics, i.e., we focus on the optical Bloch equations using the Markovian master equation in the secular approximation, given by Eq. (3.39), where the decay rates are replaced by their stationary Markovian values. The optical Bloch equations in this case are

$$\frac{d}{dt}\mathbf{R} = \mathrm{M}\mathbf{R} + \mathbf{v}, \tag{4.12}$$

where the matrix

$$\mathrm{M} = \begin{pmatrix} -\frac{1}{2}[\gamma_- + \gamma_+ + 4\gamma_0] & \omega & 0 \\ -\omega & -\frac{1}{2}[\gamma_- + \gamma_+ + 4\gamma_0] & 0 \\ 0 & 0 & -(\gamma_+ + \gamma_-) \end{pmatrix} \tag{4.13}$$

and the vector

$$\mathbf{v} = (0, 0, \gamma_- - \gamma_+). \tag{4.14}$$

Since we are using the Markovian, time-independent steady-state values for the decay rates and since in the secular approximation only two equations are coupled one can find analytical solutions to the Markovian optical Bloch equations:

$$S_x(t) = e^{-t/\tau_D}[S_{x,0}\cos\omega t - S_{y,0}\sin\omega t], \tag{4.15}$$

$$S_y(t) = e^{-t/\tau_D}[S_{y,0}\cos\omega t + S_{x,0}\sin\omega t], \tag{4.16}$$

$$S_z(t) = e^{-t/\tau_R}[S_{z,0} - S_{z,\infty}] + S_{z,\infty}, \tag{4.17}$$

where $S_{i,0}$ with $i = x, y, z$ are the initial components of the Bloch vector. In Eqs. (4.15)-(4.17) we introduced the stationary value of S_z,

$$S_{z,\infty} \equiv \lim_{t\to\infty} S_z(t) = \frac{\gamma_- - \gamma_+}{\gamma_+ + \gamma_+} = \frac{2\omega\Delta}{\omega^2 + \Delta^2}, \tag{4.18}$$

and two relaxation timescales

$$\tau_D^{-1} = \frac{1}{2}[\gamma_- + \gamma_+ + 4\gamma_0], \tag{4.19}$$

$$\tau_R^{-1} = \gamma_+ + \gamma_+. \tag{4.20}$$

The parameter τ_R defines the timescale for the relaxation of the occupation probability to its stationary value. The parameter τ_D is the decoherence time, i.e., it defines the timescale for the loss of coherence of the quantum system in the eigenbasis.

$S_x(t)$ and $S_y(t)$ undergo damped oscillations at frequency ω with damping rates τ_D^{-1}, given by Eq. (4.20). The oscillations average out in the dynamics of the norm and therefore in the dynamics of the von Neumann entropy. The stationary states for S_x and S_y are zero, and $S_z(t)$ decays exponentially form its initial value to its stationary value with decay rate τ_R^{-1}, given by Eq. (4.19).

Dynamics in the Atomic Basis

Figure 4.1 shows the dynamics of $S_z'(t)$, i.e., of the difference between the excited and ground state populations of the atomic levels. As expected, in the atomic basis we can see the damped Rabi oscillations in the components of the Bloch vector that corresponds to the population inversion. The Rabi oscillations originate from the interaction of the atom with the laser and are damped because of the presence of the environment. The non-Markovian oscillations are negligible compared to the Rabi oscillations. Therefore it is more instructive to study the non-Markovian effects in the eigenbasis of the system.

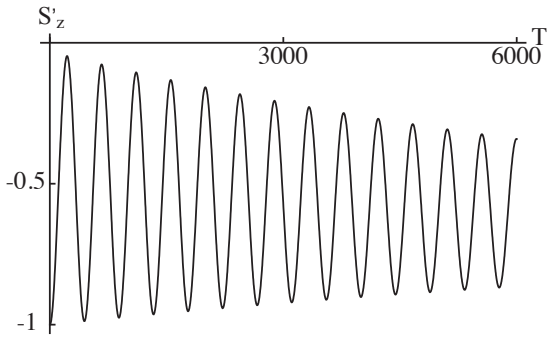

Figure 4.1: The Rabi oscillations of the $S'_z(T)$ component of the Bloch vector in the atomic basis as a function of $T = \omega_A\, t$ and with $\Delta = 0.01\,\omega_A$, $\omega_C \approx 0.2\,\omega_A$, $\Omega = 0.01\,\omega_A$ and $\alpha = 0.01$.

The Relaxation Time

It is useful to look in more detail to the relationship between the relaxation time τ_R and the decoherence time τ_D.

Consider the relaxation time

$$\begin{aligned} \tau_R^{-1} &= \gamma_- + \gamma_+ = \Big[\big(\frac{\Delta-\omega}{2\omega}\big)^2 + \big(\frac{\Delta+\omega}{2\omega}\big)^2\Big]\gamma \\ &= \frac{1}{2}\Big[1 + \frac{\Delta^2}{\Delta^2+\Omega^2}\Big]\gamma \\ &\equiv f(x)\,\gamma. \end{aligned} \tag{4.21}$$

The coefficient $f(x) \in [\frac{1}{2}, 1]$ for all values of $x = \frac{\Delta}{\Omega}$ and therefore the order of magnitude of the relaxation time is determined by the Markovian value of the decay rate

$$\tau_R^{-1} = \mathcal{O}(\gamma), \tag{4.22}$$

where

$$\begin{aligned} \gamma &= \gamma_O = \alpha\,\pi\,\omega_L\, e^{-\omega_L/\omega_C}, \quad \text{or} \\ \gamma &= \gamma_L = \frac{\alpha}{2}\frac{\Lambda^2}{\delta^2+\Lambda^2}, \end{aligned} \tag{4.23}$$

depending on which spectral density of the environment, Ohmic or Lorentzian respectively, is used.

A similar study on the decoherence time yields

$$\begin{aligned}
\tau_D^{-1} &= \frac{1}{2}\big[\gamma_- + \gamma_+ + 4\gamma_0\big] \\
&= \frac{1}{2}\Big[\big(\frac{\Delta-\omega}{2\omega}\big)^2 + \big(\frac{\Delta+\omega}{2\omega}\big)^2 + 4\big(\frac{\Omega}{2\omega}\big)^2\Big]\gamma \\
&= \frac{1}{4}\Big[1 + \frac{\Delta^2+2\Omega}{\Delta^2+\Omega^2}\Big]\gamma \\
&\equiv g(x)\,\gamma, \qquad (4.24)
\end{aligned}$$

where $g(x) \in [\frac{1}{2}, \frac{3}{4}]$ for all values of $x = \frac{\Delta}{\Omega}$. Therefore we conclude that

$$\tau_D^{-1} = \mathcal{O}(\gamma). \qquad (4.25)$$

Anastopoulos and Hu [45] have shown that the relaxation and decoherence times are of the same order of magnitude for a two-state system interacting with a zero temperature reservoir with memory. When we transform from the eigenbasis of the system back to the atomic basis, the order of magnitude for the relaxation and decoherence times is unchanged. Therefore we can conclude that the result of Anastopoulos and Hu holds also in our case when the atom is driven by a laser and the interaction between the atom and the laser is sufficiently weak.

4.3 Non-Markovian Dynamics

The definition of non-Markovian dynamics is elusive and still controversial. It has been proven that any local in time master equation can be written in a operatorial form similar to the Lindblad form, but with time dependent coefficients [46]. If the time dependent coefficients are always positive, at each moment of time the master equation is in a Lindblad form and the dynamics can be described in terms of the standard quantum jump process. This type of dynamics has been referred to as

Lindblad-type dynamics or time-dependent Markovian dynamics [47]. Here we will refer to this situation as Lindblad-type dynamics.

When the time-dependent decay rates attain negative values, for certain intervals of time, one has a more distinct non-Markovian dynamics and the effects of the reservoir memory change radically the quantum jump description. In this case we will talk about non-Lindblad-type dynamics.

When we concentrate on the small time scale dynamics of the optical Bloch equations (4.12) we must replace the Markovian stationary decay rates of Eqs. (4.13) and (4.14) with the time-dependent decay rates of Eqs. (3.50) or (3.57), depending on which spectral density, Ohmic or Lorentzian, respectively, is used to model the environment. The complicated form of the time-dependent decay rates means that the optical Bloch equations no longer yield an analytical solution and the dynamics have to be studied numerically.

Validity of the Markovian Approximation

The reservoir correlation time for the Ohmic reservoir is defined by $\tau_C^{-1} = \omega_C$. By definition the Markovian approximation is valid when $\tau_R \ll \tau_C$. Using the result of the previous section, $\tau_R^{-1} = \mathcal{O}(\gamma)$, this implies that the Markovian approximation is valid whenever

$$\alpha\,\pi\,\frac{\omega_L}{\omega_C}\,e^{-\omega_L/\omega_C} \ll 1. \tag{4.26}$$

The bound is easily satisfied in the weak coupling limit $\alpha \ll 1$, since a function of the form $o(x) = x\,e^{-x} \leq e^{-1} \approx 0.37$ for all values of $x = \frac{\omega_L}{\omega_C} \geq 0$. This means that in the weak coupling limit the Markovian approximation works well for the Ohmic spectral density.

For the Lorentzian reservoir the reservoir correlation time is $\tau_C^{-1} = \Lambda$ and the Markovian approximation is valid when

$$\frac{\alpha}{2}\frac{\Lambda^2}{\delta^2 + \Lambda^2} \ll \Lambda. \tag{4.27}$$

The weak coupling limit for the Lorentzian reservoir means that the coupling constant α is much smaller than all other relevant frequencies. This implies that $\alpha \ll \Lambda$. Therefore the Markovian approximation in the weak coupling limit works well for the Lorentzian spectral density, because a function of the form $l(x) = \frac{1}{1+x^2} \in [0, 1]$ for all values of $x = \frac{\delta}{\Lambda}$.

The strongest non-Markovian effects and non-Lindblad type dynamics appear when the decay rates attain temporarily negative values. For the Lorentzian spectral density this happens when $\delta \lesssim 3.5\Lambda$. It implies that $l(x) \lesssim 0.1$, i.e., the reservoir correlation time is many orders of magnitude smaller than the relaxation timescale, and the Markovian approximation is easily justified. A similar result holds for the Ohmic case.

This seemingly paradoxical result can be understood in the following way. The parameters that define the dynamics of the decay rates have a twofold effect on the non-Markovian dynamics of the system. On one hand, they determine the timescales for both the memory effects and the relaxation dynamics. On the other hand, they also determine the amplitude of the oscillations of the decay rate around its stationary value and whether the decay rate attains negative values or nor. These two effects are not independent and for both types of reservoirs, the Ohmic and the Lorentzian, we find that when the *amplitude* of the non-Markovian oscillations is increased, then the *timescale* for the non-Markovian effects is decreased.

In general the decay rates are dependent on the coupling constant α, which describes the strength of the coupling between the system and the environment. Therefore in the weak coupling limit the non-Markovian effects are very small compared to the relaxation dynamics. To enhance the non-Markovian effects one needs to extend the master equation of the two-state system to include the effect of stronger coupling between the system and the environment, e.g., by considering higher order terms in the expansion of the TCL generator of Eq. (2.66).

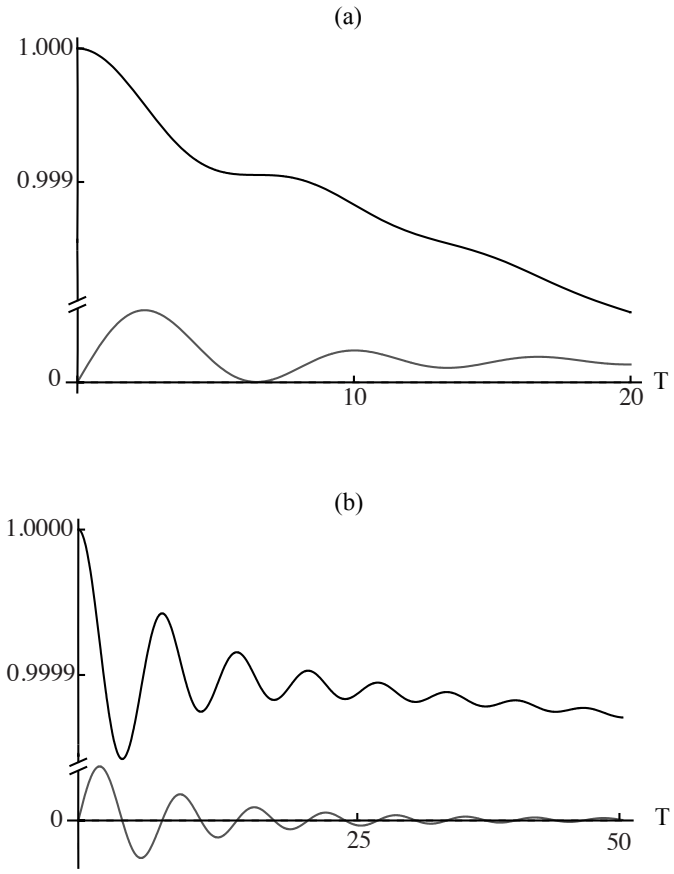

Figure 4.2: The non-Markovian dynamics of the $S_z(T)$-component of the Bloch vector in an Ohmic reservoir as a function of $T = t\,\omega_A$ with $\Delta = 0$, $\Omega = 0.01\,\omega_A$, $\alpha = 0.01$ and for (a) $\omega_C = 0.1\,\omega_A$ and for (b) $\omega_C = 0.2\,\omega_A$. The black line is $S_z(T)$ and the gray line is the Ohmic decay rate $\gamma_O(T)$ (not in scale).

Effect of the Decay Rate on the Non-Markovian Dynamics

In Sec. 3.4 we have seen how the dynamics of the decay rates essentially determine the non-Markovian dynamics of the system. This is confirmed in Fig. 4.2 where the non-Markovian dynamics of the z-component of the Bloch vector in the eigenbasis is plotted in the Ohmic case for two decay rates corresponding to the Lindblad type and non-Lindblad type regimes. The initial state is $\mathbf{R}(0) = (0, 0, 1)$ and therefore the dynamics of the Bloch vector is completely characterized by $S_z(t)$, since $S_{x,y}(t) = S_{x,y}(0) = 0$ for all times t.

When the decay rate is positive the value of $S_z(t)$ decreases, but since the decay rate is not constant at short times, the decay is not exponential, as it would be in the Markovian case [48]. When the decay rate attains negative values, the value of $S_z(t)$ increases, indicating that energy is flowing back from the environment into the system. For this initial state the norm of the Bloch vector is $\|\mathbf{R}(t)\| = |S_z(t)|$ and we can conclude that the same non-Markovian oscillations appear in the dynamics of the norm and therefore in the dynamics of both the purity, given by Eq. (4.4), and the von Neumann entropy, given by Eq. (4.5). In particular when the decay rate is negative the von Neumann entropy decreases, indicating that also information is flowing from the environment to the system.

It is clear from Fig. 4.2 that when the values of the decay rate deviate most from their stationary values, the non-Markovian effects are most visible. However, it is also apparent that the non-Markovian effects are very small, $\mathcal{O}(10^{-3})$ for the Lindblad type case of Fig. 4.2 (a) and $\mathcal{O}(10^{-4})$ for the non-Lindblad type case of Fig. 4.3 (b) whereas the effect of the relaxation is $\mathcal{O}(1)$. This is in accordance with the observations of the previous section, i.e., in general the non-Markovian effects appear on small timescales compared to the relaxation timescale and in particular, the timescale is smaller for the non-Lindblad type dynamics than for the Lindblad-type dynamics. The results of this section are not restricted to the chosen initial

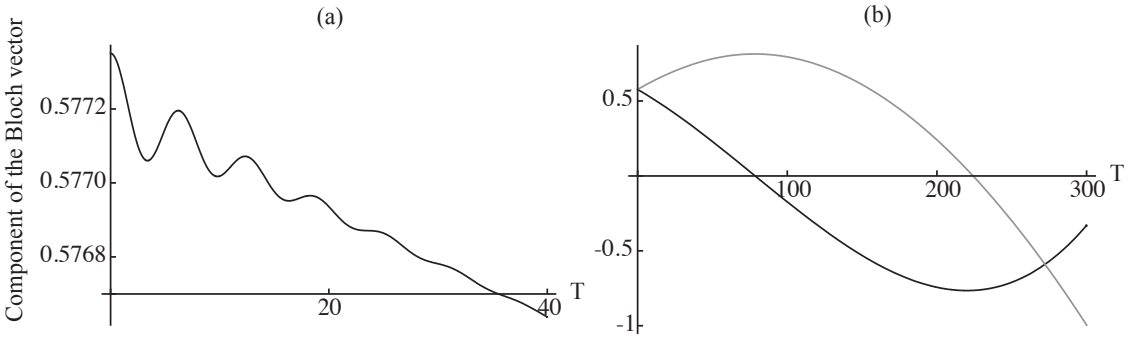

Figure 4.3: The non-Markovian dynamics of (a) the $S_z(t)$-component and (b) the $S_x(t)$ (black line) and the $S_y(t)$ (gray line) components of the Bloch vector in a Lorentzian reservoir as a function of $T = t\,\omega_A$ with $\Delta = 0$, $\Omega = 0.01\,\omega_A$, $\delta = \omega_A$, $\Lambda = 0.1\,\omega_A$ and $\alpha = 0.001\,\omega_A$.

state nor to the Ohmic reservoir. Similar dynamics of the Bloch vector and of the von Neumann entropy can be seen for other initial conditions and in the case of a Lorentzian reservoir. As an example, in Fig. 4.3 we show the dynamics of the Bloch vector for a reservoir with a Lorentzian spectral density and with an initial state $\mathbf{R}(0) = \frac{1}{\sqrt{3}}(1,1,1)$. We can see that the non-Markovian effects are strongest for $S_z(t)$. For $S_x(t)$ and $S_y(t)$ the non-Markovian oscillations are negligible in comparison to the large oscillations caused by the interaction with the driving laser. The non-Markovian oscillations appear in the norm of the Bloch vector and are therefore reflected in the dynamics of the von Neumann entropy.

Effect of the Laser Amplitude and Detuning on the Non-Markovian Dynamics

Both the detuning $\Delta = \omega_A - \omega_L$ and the Rabi frequency Ω affect the amplitude of the non-Markovian oscillations. The combined effect of the laser parameters is most clearly understood when we look at the equation of motion of $S_z(t)$:

$$\frac{d}{dt}S_z(t) \propto -[\gamma_+(t) + \gamma_-(t)]S_z(t) = -f(x)\gamma(t)S_z(t) \tag{4.28}$$

where $f(x) = 1 - \frac{1}{2(1+x^2)}$ and $x = \frac{\Delta}{\Omega}$. It is clear that the changes is $S_z(t)$ are proportional both to the value of $\gamma(t)$ and to $f(x)$.

When the detuning is constant and the laser amplitude is decreased, the amplitude of the non-Markovian oscillations increases (see Fig. 4.4 (a)). In a similar manner when Ω is constant and the laser detuning is increased, the amplitude of the non-Markovian oscillations increases (see Fig.4.4 (b)). However, it is worth noting that the effect of changing the frequency of the laser, ω_L, and hence the detuning Δ, is more complicated than the effect of changing the laser amplitude, and hence Ω, because the decay rates of Eqs. (3.41)-(3.44) are dependent on the value of ω_L for all kinds of reservoirs. In other words the dynamics does not depend simply on the ratio $x = \frac{\Delta}{\Omega}$ but on Δ and Ω separately.

Overall, the effect of the laser amplitude and detuning on the non-Markovian dynamics is not very large and we conclude that the laser neither damps nor enhances the memory effects considerably.

4.4 Full Dynamics of the Driven Two-State System

So far the dynamics of the driven two-state have been studied using the master equation in the secular approximation. The effect of the non-secular terms is non-

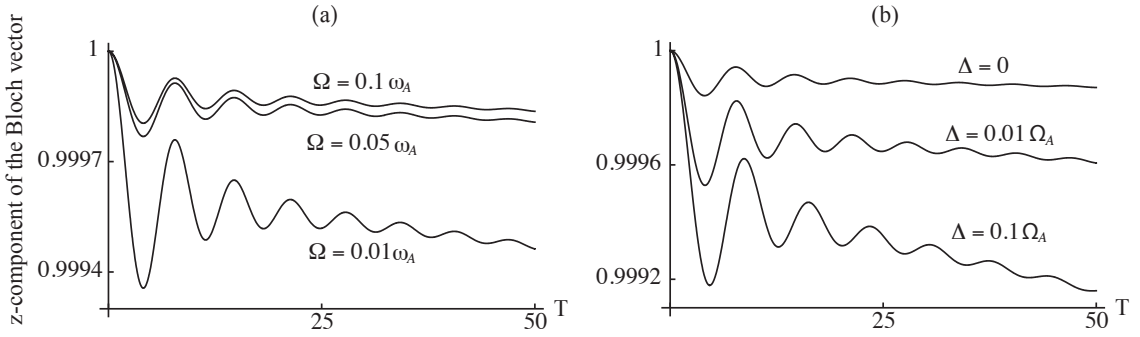

Figure 4.4: The effect of (a) Ω and (b) Δ on the non-Markovian oscillations of the $S_z(T)$-component of the Bloch vector in an Ohmic reservoir with $T = t\,\omega_A$, $\omega_C = 0.1\,\omega_A$ and $\alpha = 0.01$. In (a) $\Delta = 0.01\,\omega_A$ and (b) $\Omega = 0.01\,\omega_A$.

trivial, especially from the point of view of the non-Markovian dynamics, and it turns out to be interesting, as we will see in this last section. Therefore it is important to consider the full master equation.

Validity of the Secular Approximation

By definition the secular approximation is valid when $\tau_S \ll \tau_R$, where $\tau_S^{-1} = \omega = \sqrt{\Delta^2 + \Omega^2}$ and $\tau_R^{-1} = \mathcal{O}(\gamma)$. This implies, for the Ohmic case, that

$$\alpha\,\pi\,\omega_L e^{-\omega_L/\omega_C} \ll \omega. \tag{4.29}$$

Since $\alpha \ll 1$ but $\omega \ll \omega_L$, the validity of the secular approximation for the Ohmic case is strongly dependent on the particular choice of parameters Ω and Δ as well as on the cut-off frequency ω_C:

(SI) If $\omega_C \ll \omega_L$, ω_A then $e^{-\omega_L/\omega_C} \ll 1$ and the secular approximation is more likely to be a good approximation, i.e., $\tau_S \ll \tau_R$.

(SII) If $\omega_C \approx \omega_L$, ω_A, then the separation of the timescales becomes ambiguous, i.e., $\tau_S \sim \tau_R$.

When the reservoir is Lorentzian, the secular approximation is valid when

$$\frac{\alpha}{2}\frac{\Lambda^2}{\delta^2+\Lambda^2} \ll \omega. \tag{4.30}$$

Since $l(x) = \frac{1}{1+x^2} = \mathcal{O}(1)$ for all values of $x = \frac{\delta}{\Lambda}$, this condition implies $\alpha \ll \omega$, which is trivially satisfied in the weak coupling regime.

However, it is important to notice that the secular approximation only coarse grains the effect of the non-secular terms on the time scale of the relaxation processes. In a non-Markovian study of the dynamics we must also compare the typical time scale to the reservoir correlation time. Consider, e.g., the two cases SI and SII described above. For the case (SI) the reservoir correlation time is $\tau_C^{-1} = \omega_C \ll \omega_L$, ω_A and the typical timescale of the system is $\tau_S^{-1} = \omega \ll \omega_L$, ω_A. Therefore the non-Markovian and the non-secular effects happen on similar timescales, i.e., $\tau_C \sim \tau_S$. For the case (SII) we find that $\tau_C \ll \tau_S$ and there is a clear distinction between the time scales of non-Markovian and non-secular effects, i.e., $\tau_C \ll \tau_S$.

4.4.1 Full Optical Bloch Equations

The study of the non-secular terms requires a derivation of the optical Bloch equations using the full master equation (3.58). The full optical Bloch equations are

$$\frac{d}{dt}\mathbf{R} = (\mathrm{M} + \mathrm{M_{NS}})\mathbf{R} + \mathbf{v} + \mathbf{v}_{\mathrm{NS}}, \tag{4.31}$$

where M and $\mathbf{v}$ are defined in Eq. (4.13) and Eq. (4.14). The effect of the non-secular terms is contained in both the matrix

$$\mathrm{M_{NS}} = \begin{pmatrix} -\gamma(t)(\frac{\Omega}{2\omega})^2 & 0 & \gamma(t)\frac{\Delta\Omega}{2\omega^2} \\ 0 & \gamma(t)(\frac{\Omega}{2\omega})^2 & \lambda(t)\frac{\Omega}{\omega} \\ \gamma(t)\frac{\Delta\Omega}{2\omega^2} & -\lambda(t)\frac{\Omega}{\omega} & 0 \end{pmatrix} \tag{4.32}$$

and the vector

$$\mathbf{v}_{\mathrm{NS}} = (\gamma(t)\frac{\Omega}{\omega}, 0, 0). \tag{4.33}$$

The equation of motion of the components of the Bloch vector are all coupled to each other and they depend on the $\lambda(t)$-decay rate, i.e., the imaginary part of Eq. (2.35), as well as on the $\gamma(t)$-decay rate, i.e., the real part of Eq. (2.35).

Interestingly, when the stationary state of the Bloch vector in the eigenbasis is computed using the full optical Bloch equations, all three components are non-zero. Recall that the stationary solution of the secular approximated master equation (4.12) is $\mathbf{R} = (0, 0, S_{z,\infty})$. This shows that the secular approximation is not simply a coarse graining of the dynamics. Indeed, if we neglect the non-secular terms based on the fact that they average out for times longer than the typical time scale of the system, we also affect the stationary value of the Bloch vector.

This result, i.e., that the secular approximation has an effect on the stationary values of the components of the Bloch vector agrees with the work of Kowalewska-Kudłaszyk and Tanaś, who also derived their master equation microscopically [36, 37].

In the next section we proceed to show the effects of the non-secular terms using the solution of the full optical Bloch equations of Eq. (4.31) and comparing them with the solutions of the secular approximated optical Bloch equations of Eq. (4.12).

4.4.2 Full Dynamics of the Bloch Vector

The standard textbook approach to the secular approximation comprises of neglecting terms that oscillate very rapidly during the time τ_R, i.e., the relaxation time of the system. The secular approximation is said to be valid whenever $\tau_S \ll \tau_R$, where τ_S is the typical time scale of the system [1]. This definition, however, fails to mention that the non-secular terms can also affect the stationary state of the system.

In Fig. 4.5 we present the dynamics of the components and the norm of the Bloch vector using the Ohmic spectral density and parameters that correspond to

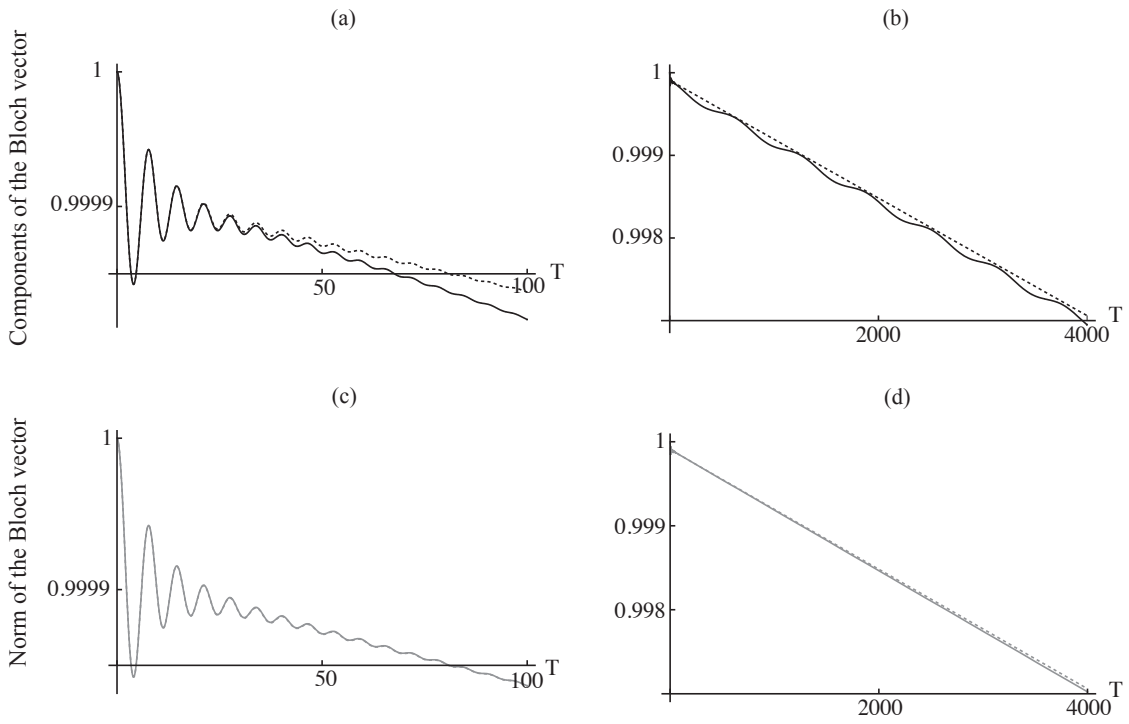

Figure 4.5: A comparison between the time-evolution of (a)-(b) the $S_z(T)$-component and (c)-(d) the norm of the Bloch vector in the Ohmic reservoir for (a) and (c) short times and for (b) and (d) longer times, calculated with (dashed line) and without (full line) the secular approximation. The values of the parameters are $\Delta = 0$, $\omega_C = 0.1\,\omega_A$, $\Omega = 0.01\,\omega_A$ and $\alpha = 0.01$.

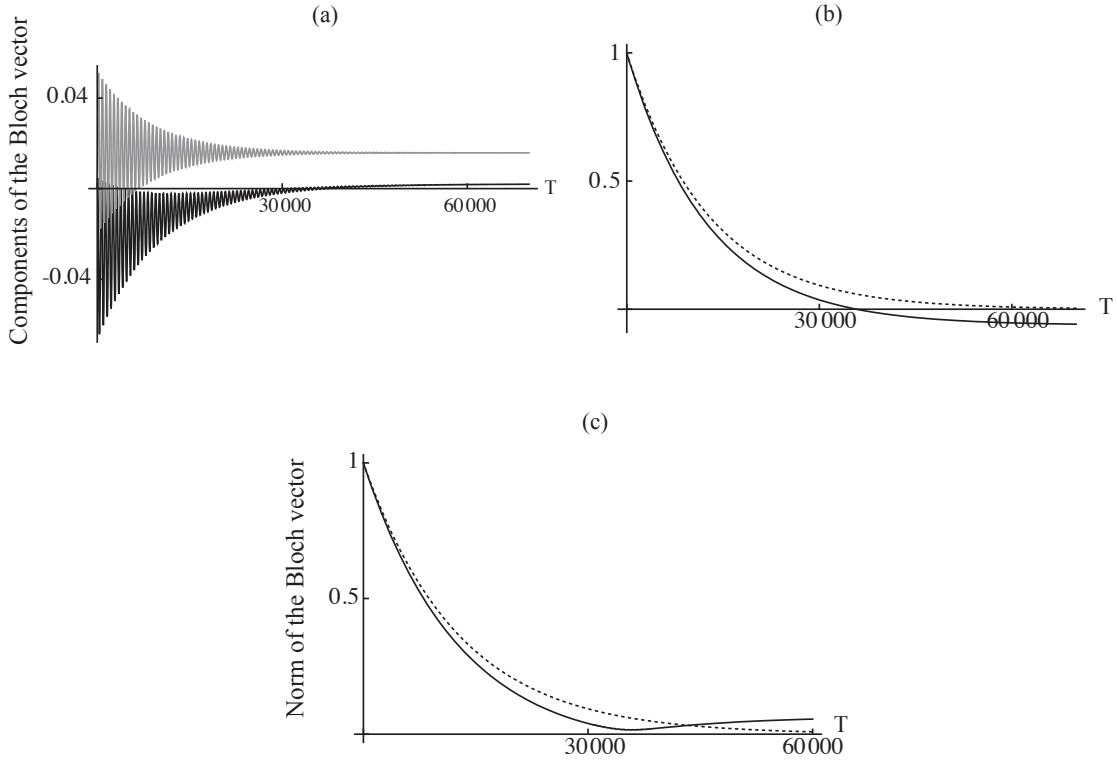

Figure 4.6: Relaxation dynamics of (a) the $S_x(T)$ (black line) and the $S_y(T)$ (gray line) components, (b) the $S_z(T)$-component and (c) the norm of the Bloch vector in an Ohmic reservoir with $T = t\,\omega_A$, $\Delta = 0$, $\omega_C = 0.2\,\omega_A$, $\Omega = 0.01\,\omega_A$ and $\alpha = 0.01$.

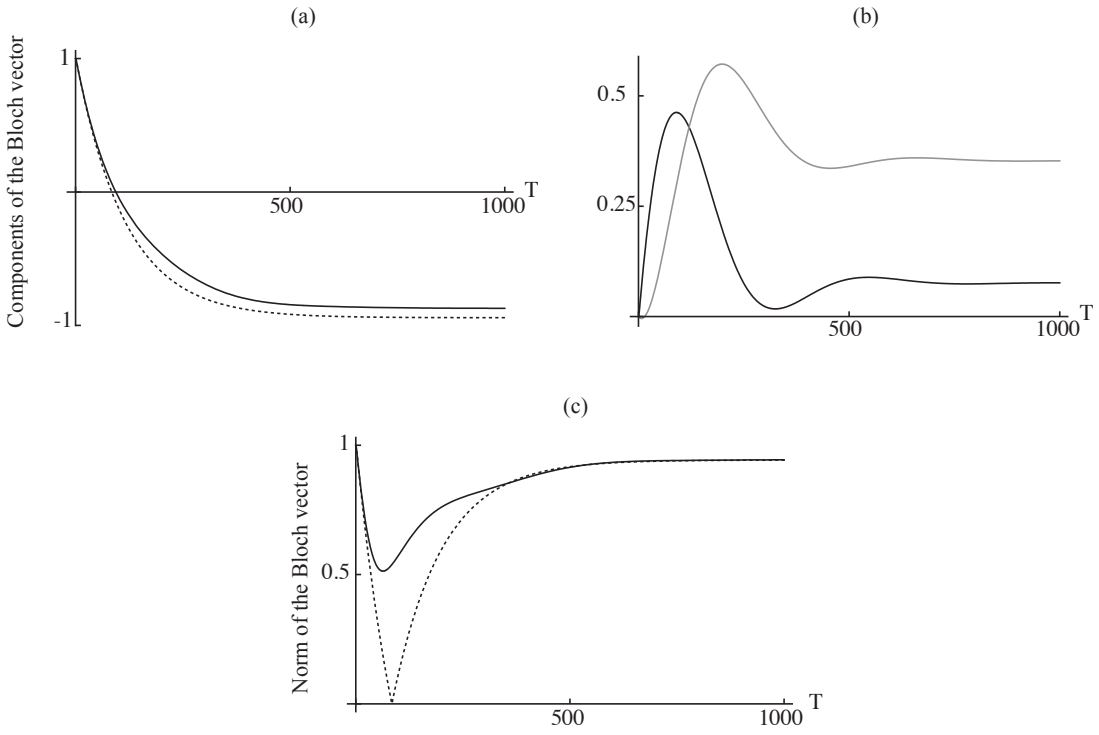

Figure 4.7: The relaxation dynamics of (a) the $S_z(T)$-component, (b) the $S_x(T)$ (black line) and $S_y(T)$ (gray line) components and (c) the norm of the Bloch vector in the Ohmic reservoir calculated with (dashed line) and without (full line) the secular approximation. The values of the parameters are $\Delta = 0.01\,\omega_A$, $\omega_C = \omega_A$, $\Omega = 0.01\,\omega_A$ and $\alpha = 0.01$.

$\tau_C \sim \tau_S \ll \tau_R$, i.e., when we are in the regime specified by case (SI). According to the textbook definition we would, in this case, expect the secular approximation to hold.

The effect of the non-secular terms on the non-Markovian oscillations of $S_z(t)$ is shown in Fig. 4.5 (a). For very short times, $t = \mathcal{O}(\tau_C)$, the full and the secular approximated solutions of S_z coincide. The deviations begin to appear for $t \simeq \tau_S$. Since the non-secular oscillations affect the non-Markovian time evolution, we conclude that if one is interested in the short time scale dynamics the non-secular terms must be taken into account also when $\tau_S \ll \tau_R$.

Figure 4.5 (b) shows long-time dynamics of $S_z(t)$ for times $t \geq \mathcal{O}(\tau_S)$. The solution of the full optical Bloch equations (4.31) oscillates while the solution of the secular approximated optical Bloch equations (4.12) decays steadily. The differences between the two solutions are small, $\mathcal{O}(10^{-3})$, and they are negligible on the time scale of the relaxation.

In Fig. 4.5 (c) we see that the non-Markovian oscillations appear in the norm of the Bloch vector and therefore they are reflected in the purity and the von Neumann entropy function. The non-secular oscillations, however, do not contribute to the dynamics of the norm of the Bloch vector, as can be seen in Fig. 4.5 (d). Therefore the non-secular terms do not affect the dynamics of the von Neumann entropy or the purity of the system. This implies that the non-secular effects differ physically from the non-Markovian effects.

Finally, Fig. 4.6, shows the difference between the secular and exact dynamics of the Bloch vector components and for the norm of the Bloch vector for times $t = \mathcal{O}(\tau_R)$. It is worth pointing out that the initial state of the system is $\mathbf{R} = (0, 0, 1)$ and in the secular approximation $S_i(t) = S_i(0) = 0$ for $i = x, y$ and for all times t. We observe that the non-secular terms affect also the stationary values of the quantities. Indeed the stationary states of the secular approximated and of the full optical

Bloch equations do not, in general, coincide.

The difference between the stationary states of the full and of the approximated solutions is small but significant from the point of view of the physical implications. For example, in the case of exact resonance, such as in Fig. 4.6, the stationary state obtained as the solution of the approximated master equation (3.39) corresponds to a maximally mixed state. However, the stationary solution of the full master equation corresponds to a Bloch vector with a non-zero norm, implying a smaller degree of mixedness.

The solutions of the optical Bloch equations (4.12) and (4.31), i.e., the approximated and the full optical Bloch equations, respectively, are plotted in Fig. 4.7 for parameters corresponding to the case (SII). In that case $\tau_C \lesssim \tau_S \lesssim \tau_R$ and the time scales are not distinct. In this case, as we mentioned, we do not expect the secular approximation to hold and indeed the differences between two solutions are large.

The results of this section have been obtained by studying the time-evolution of the Bloch vector in the Ohmic reservoir. However, similar results also hold for the Lorentzian reservoir. The difference that comes from the choice of the reservoir spectrum is most pronounced when $t = \mathcal{O}(\tau_C)$, i.e. in the non-Markovian time scale. When the decay rates reach their stationary values the dynamics of the Bloch vector, for the Ohmic and the Lorentzian reservoirs, can be predicted qualitatively from the dynamics of the decay rates corresponding to the two different spectra. Because the decay rates have very similar dynamics, consequently they induce similar dynamics on the two-state system.

4.4.3 Dynamics of the Bloch Sphere

The dynamics of the Bloch vector is, of course, dependent on the initial state of the system. For example, a general view of the time evolution of all pure initial states can be considered simultaneously by studying the dynamics of the entire Bloch

sphere. In general dissipation of energy and information from the system to the environment causes the Bloch sphere to deform into an ellipsoid and to shrink towards a stationary state. During the non-Markovian time scale the ellipsoid can pulsate due to the temporary increase in the excited state population and/or recoherence, caused by memory effects; the driving laser on the other hand causes the ellipsoid to rotate around the z-axis.

The dynamics of the states initially on the Bloch sphere are presented for two different exemplary sets of parameters in Fig. 4.8 and Fig. 4.9. When $\Delta = 0$ the stationary state lies near the origin (See Fig 4.8). However, due to the effect of the non-zero stationary values of the non-secular terms. Therefore the stationary state in this case is slightly displaced from the origin, and the mapping corresponding to the time evolution is not unital, i.e., in Eq. (4.7) the translation vector $\mathbf{v} \neq 0$.

For parameter values used in Fig. 4.8 the relaxation time τ_R of Eq. (4.19) and the decoherence time τ_D of Eq. (4.20) are such that $\tau_R = \frac{3}{2}\tau_D$. Therefore the Bloch vector components S_x and S_y are damped more rapidly than the component S_z. This explains why the Bloch sphere evolves into an ellipsoid that is squeezed along the x- and y-axes.

When the detuning Δ is increased the stationary state moves further away from the origin, approaching the point $(0, 0, -1)$ in the limit $\frac{\Omega}{\Delta} \to 0$. This point corresponds to the pure state $|g\rangle$. An exemplary case of $\Delta \neq 0$ is shown in Fig. 4.9. In this case we find that $\tau_R = \frac{5}{6}\tau_D$. Therefore the Bloch vector component S_z is damped more rapidly than S_x and S_y and the Bloch sphere evolves into an ellipsoid that is squeezed along the z-axis.

For a non-zero detuning the stationary state is close to the South pole of the Bloch ball and the dynamics for states initially in the northern hemisphere differ from the dynamics for states initially in the southern hemisphere. As an extreme example, Fig. 4.10 shows the individual trajectory of a single Bloch vector initially

in the North pole. The Bloch vector passes through the origin and simultaneously its entropy peaks at its maximal value $\log 2$. As the Bloch vector approaches its stationary state the norm increases and the entropy falls. The Bloch vector initially in the South pole only exhibits a small decrease in its norm and a small increase in its entropy (figure 4.11).

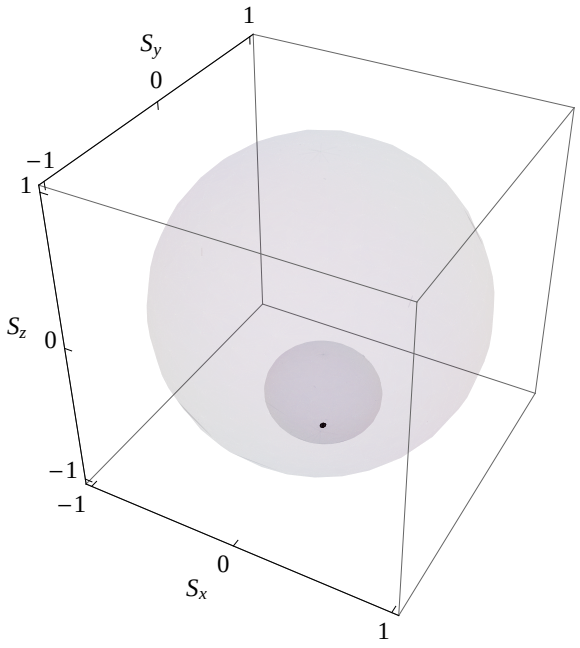

Figure 4.8: Dynamics of initially pure states in the Bloch ball in the Ohmic reservoir for times $T = 0$ (light gray sphere), $T = 10\,000$ (dark gray ellipsoid) and $T = 45\,000$ (black point) with $T = \omega_A t$, $\Delta = 0$, $\Omega = 0.01\,\omega_A$, $\omega_C = 0.1\,\omega_A$ and $\alpha = 0.01$.

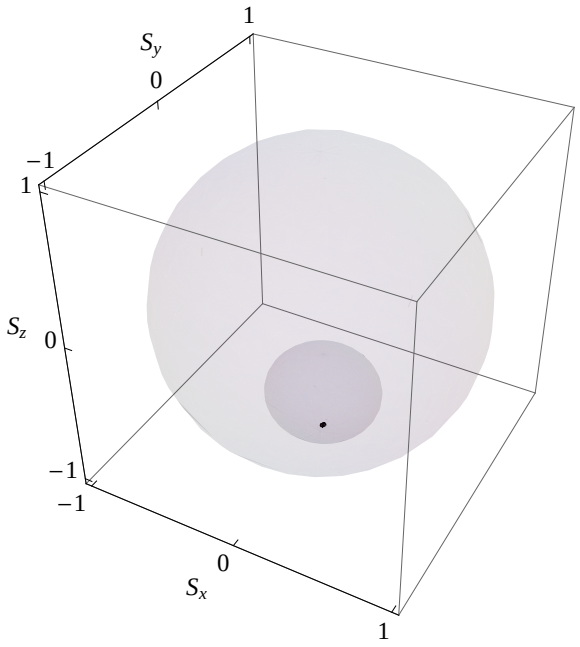

Figure 4.9: Dynamics of initially pure states in the Bloch Ball in the Ohmic reservoir for times $T = 0$ (light gray sphere), $T = 10\,000$ (dark gray ellipsoid) and $T = 40\,000$ (black point) with $T = \omega_A\, t$, $\Delta = 0.01\,\Omega_A$, $\Omega = 0.01\,\omega_A$, $\omega_C = 0.1\,\omega_A$ and $\alpha = 0.01$.

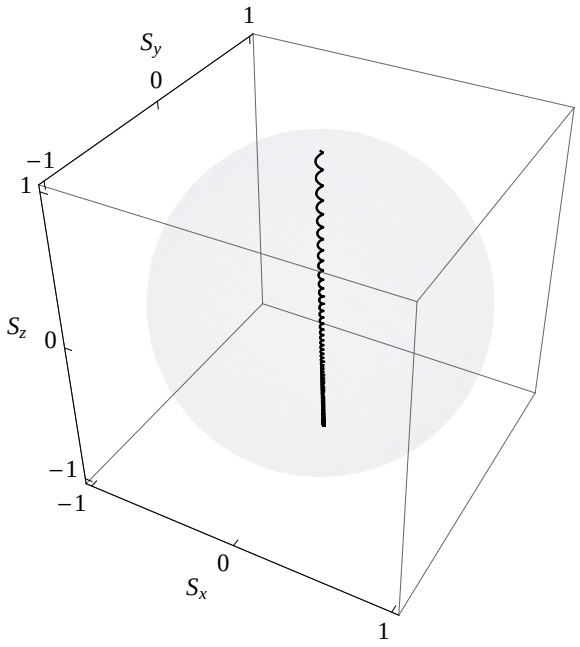

Figure 4.10: An individual trajectory of the Bloch vector with $\Delta = 0.01\,\omega_A$, $\omega_C = 0.2\,\omega_A$, $\Omega = 0.01\,\omega_A$ and $\alpha = 0.01$. The gray unit ball is the state space $\mathcal{S}(\mathcal{H})$ of two-state systems.

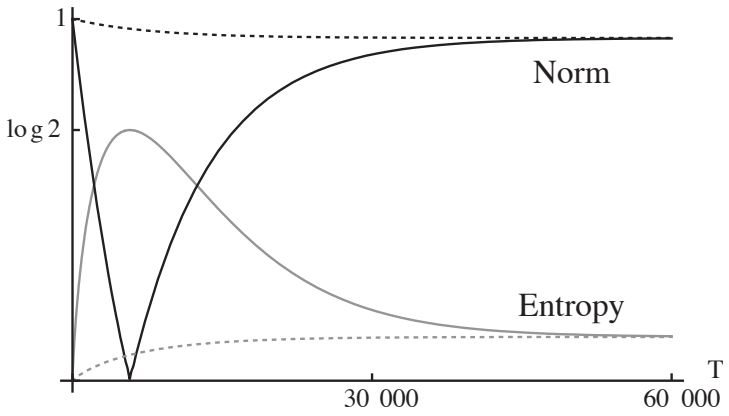

Figure 4.11: The norm (black line) and the von Neumann entropy (gray line) of a Bloch vector for two initial states $\mathbf{R} = (0, 0, 1)$ (full line) and $\mathbf{R} = (0, 0, -1)$ (dashed line) with $\Delta = 0.01\,\omega_A$, $\omega_C = 0.2\,\omega_A$, $\Omega = 0.01\,\omega_A$ and $\alpha = 0.01$.

Chapter 5

Conclusions

In this thesis we have derived a non-Markovian local-in-time master equation for a two-state system interacting both with a driving laser and with a structured reservoir at zero temperature. We have obtained the master equation using the time-convolutionless projection operator method in the limit of weak coupling between the system and the environment. The master equation contains the unitary evolution of the two-state system which is disrupted by quantum jumps between the eigenstates of the system and by phase flips. The combined effect of the quantum jumps and the phase flips is to dissipate and decohere the system.

The effect of the non-trivial structure of the reservoir is reflected in the time-dependence of the decay rates. When the decay rates deviate considerably from their stationary Markovian values the dynamics of the system cannot be described by a Markovian master equation. The decay rates essentially determine the non-Markovian dynamics of the two-state system. In particular, when the decay rates attain temporarily negative values the reservoir memory effects become evident and the direction of the quantum jumps is reversed. The reversed jumps can lead to recoherence of the system as well as a reversed flow of information and energy back to the system from the environment.

In this study the non-Markovian dynamics were considered using two different spectral densities of the environment, i.e., an Ohmic spectral density and a Lorentzian spectral density. Both of these reservoirs induced qualitatively similar non-Markovian dynamics. In the weak coupling limit the non-Markovian time scale is very small compared to the time scale for the relaxation dynamics and the Markovian approximation works well for both reservoirs under consideration. A natural continuation to the work of this thesis is an extension of the master equation to the regime of stronger coupling between the system and the environment. In the strong coupling regime the non-Markovian effects are expected to be more significant compared to the relaxation dynamics. Moreover, a more general master equation can give new physical insight into the non-Markovian dynamics of the driven damped two-state system.

In addition to the unitary evolution and the quantum jumps and phase flips the dynamics of the system contains the effect of the so-called non-secular terms. The non-secular terms are often neglected in the secular approximation. When the typical time scale of the system is small compared to the relaxation time scale, the non-secular terms oscillate very rapidly and the oscillations average out.

However, the non-secular terms also affect the state of the system for long time scales. In particular, the stationary state of a two-state system can be considerably different with and without the secular approximation. These differences are reflected in quantities such as the purity and the von Neumann entropy, describing the statistical properties of the two-state system. Moreover, for non-Markovian time scales the non-secular terms can be very significant, because generally the time scales for these two effects, i.e., the non-Markovian effects and the non-secular effects, cannot be considered distinct. Therefore the non-secular oscillations distort the non-Markovian oscillations.

In the future we plan to extend the study of the dynamics of the damped driven

two-state system to the case of two driven qubits. In addition to interest in such a system from a fundamental point of view, the results can contribute to the study of basic logic gates in quantum computing. Moreover, it would be interesting to see how the entanglement dynamics are affected by both the driving laser and the reservoir memory effects.

Bibliography

[1] H.-P. Breuer and F. Petruccione, *The Theory of Open Quantum Systems*, Oxford University Press, Oxford (2002).

[2] U. Weiss, *Quantum Dissipative Processes*, World Scientific Publishing, Singapore (1999).

[3] E. B. Davies, *Quantum Theory of Open Systems*, Academic Press, London (1976).

[4] M. Schlosshauer, *Decoherence and the Quantum-to-Classical Transition*, Springer-Verlag, Berlin Heidelberg (2007).

[5] J. Piilo *et al.*,Phys. Rev. Lett. **100**, 180402 (2008).

[6] J. Piilo *et al.*, arXiv:0902.3609v1 [quant-ph].

[7] S. Haroche and J.-M. Raimond, *Exploring the Quantum: Atoms, Cavities and Photons*, Oxford University Press, Oxford (2006).

[8] P. Lambropoulos *et al.*, Rep. Prog. Phys. **63**, 455 (2000).

[9] M. A. Nielsen and I. L. Chuang, *Quantum Computation and Quantum Information*, Cambridge University Press, Cambridge (2000).

[10] L. Ballentine *Quantum Mechanics - A Modern Development*, World Scientific Publishing, Singapore (1998).

[11] E. P. Wigner, *Gruppentheorien*, Frederick Wieweg und Sohn, Braunschweig, Germany (1931).

[12] M. H. Stone, Ann. Math. **33**, 643 (1932).

[13] N. Dunford and J. T. Schwartz, *Linear Operators, Part I, General Theory*, Interscience Publishers, New York (1958).

[14] R. Alicki and K. Lendi, *Quantum Dynamical Semigroups and Applications*, LPN 286, Springer-Verlag, Berlin Heidelberg (1987).

[15] G. Lindblad, Commun. Math. Phys. **48**, 119 (1976).

[16] V. Gorini, A. Kossakowski and E. Sudarshan, J. Math. Phys. **17**, 821 (1976).

[17] J. Kiukas, Notes prepared for a seminar "Proof of Lindblad's theorem on the uniformly continuous quantum dynamical semigroups" (2008).

[18] W. F. Stinespring, Proc. Amer. Math. Soc. **6**, 211 (1955).

[19] J. Dalibard, Y. Castin and K. Mølmer, Phys. Rev. Lett. **68**, 580 (1992).

[20] M. B. Plenio and P. L. Knight, Rev. Mod. Phys. **70**, 101 (1998).

[21] S. Nakajima, Prog. Theor. Phys. **20**, 948 (1958).

[22] R. Zwanzig, J. Chem. Phys. **33**, 1338 (1960).

[23] F. Shibata, Y. Takahashi and N. Hashitsume, J. Stat. Phys. **17**, 171 (1977).

[24] H.-P. Breuer, B. Kappler and F. Petruccione, Ann. Phys. **291**, 36 (2001).

[25] S. Maniscalco and F. Petruccione, Phys. Rev. A **73**, 012000 (2006).

[26] A. Royer, Phys. Lett. A **315**, 335 (2003).

[27] C. Cohen-Tannoudji *et al.*, *Atom-Photon Interactions*, Wiley Science Paperback Series, New York (1998).

[28] B. R. Mollow, Phys. Rev. **188**, 1969 (1969).

[29] B. R. Mollow, Phys. Rev. A **12**, 1919 (1975).

[30] H. Carmichael and D. F. Walls, J. Phys. B **9**, 1199 (1976).

[31] H. J. Kimble and L. Mandel, Phys. Rev. A **13**, 2123 (1976) .

[32] C. Gerry and P. Knight, *Introductory Quantum Optics*, Cambridge University Press, Cambridge (2004).

[33] J. Paz and W. Zurek, Phys. Rev. Lett **82**, 5181 (1999).

[34] H. J. Carmichael *Statistical Methods in Quantum Optics 1*, Springer-Verlag, Berlin Heidelberg (2002) .

[35] B. R. Mollow and M. M. Miller, Ann. Phys. **52**, 464 (1969).

[36] A. Kowalewska-Kudłaszyk and R. Tanaś, Acta Physica Slovaca **50**, 313 (2000).

[37] A. Kowalewska-Kudłaszyk and R. Tanaś, J. Mod. Opt. **48**, 1059 (2001).

[38] A. A. Budini, J. Chem. Phys. **126**, 054101 (2007).

[39] F. Bloch, Phys. Rev. **70**, 460 (1046).

[40] A. Pasieka *et al.*, Acta Appl. Math., published online: http://www.springerlink.com/content/1097u1t485053w54/, (2009).

[41] S. Daffer, K. Wòdkiewicz and J. K. McIver, Phys. Rev. A **67**, 062312 (2003).

[42] S. Daffer, K. Wòdkiewicz and J. K. McIver, J. Mod. Opt. **15**, 1843 (2004).

[43] S. Daffer *et al.*, Phys. Rev. A **70**, 010304 (2004).

[44] S. Maniscalco, Phys. Rev. A **75**, 062103 (2007).

[45] C. Anastopoulos and B. L. Hu, Phys. Rev. A **62**, 033821 (2000).

[46] H.-P. Breuer, Phys. Rev. A **70**, 012106 (2004).

[47] M. M. Wolf *et al.*, Phys. Rev. Lett. **101**, 150402 (2008).

[48] K. K. Wòdkiewicz and J. H. Eberly, Ann. Phys. **101**, 574 (1976).